Mechanism and Machine Theory, 2019, Vol 142, 103577
https://doi.org/10.1016/j.mechmachtheory.2019.103577

Operation Mode Analysis of Lower-Mobility Parallel Mechanisms Based on Dual Quaternions

Kai Liu[a], Xianwen Kong[b], Jingjun Yu[a,*]
a. *Robotics Institute, Beihang University, Beijing 100191, China*
b. *School of Engineering and Physical Sciences, Heriot-Watt University, Edinburgh EH14 4AS, UK*
* Corresponding author, E-mail address: jjyu@buaa.edu.cn

Abstract: This paper aims to provide an efficient way for analyzing operation modes and revealing corresponding motion characteristics of lower-mobility parallel mechanisms (LMPMs) using unit dual quaternions. Unit dual quaternions are first classified into 132 cases corresponding to 132 elementary operation modes based on the number of constant zero components. Meanwhile, the kinematic interpretation of these cases is presented in detail. Then a general method for analyzing operation modes and revealing motion characteristics of LMPMs is proposed according to unit dual quaternions and geometrical constraints. By this means, operation modes of LMPMs with complicated constraint conditions can also be analyzed, where a prime decomposition of the ideal corresponding to constraint equations in this condition is infeasible. Taken a 3-RSR LMPM and a 3-RPS LMPM as examples, the operation modes and motion characteristics can be obtained by the proposed approach. It is shown that the former LMPM has seven operation modes including two elementary operation modes and five extra operation modes. Under certain operation modes, the zero-torsion motion of the 3-RSR LMPM can not even be achieved. On the other hand, the latter has two operation modes in which the parasitic motion exists. To gain a deeper insight into the physical meaning of the operation modes, axodes are analyzed and drawn by mean of the velocity operator. It is demonstrated that the 3-RSR LMPM can realize an equal-diameter spherical pure rolling movement with variable diameters and the 3-RPS LMPM can achieve a rolling movement accompanied by sliding.
Keywords: lower-mobility parallel mechanism; operation mode; geometric constraint; dual quaternion; axode

1. Introduction

Lower-mobility parallel mechanisms (LMPMs) have less than six degrees of freedom (DOF). These mechanisms, especially two-rotational and one-translational (2R1T) LMPMs, draw much attention and play an important part in tasks that do not require full rigid motions of the end-effector [1-3], e.g., positioning, symmetrical machining and alignment, etc. As a well-known LMPM, the 3-RPS LMPM, which can produce one translation and two rotations, has been used as a tool head of machine tools [4]. A satellite-tracking device has been designed based on the 3-RSR LMPM with 2R1T DOFs as well [5]. Furthermore, the 3-RSR LMPM with minor adjustments also has been used as a robot wrist [6], a wearable haptic device [7], etc.

Actually, functions and applications of LMPMs always depend on their own operation modes which were defined as a set of transformations among a continuous set of poses of the mobile platform [8-9]. Zlatanov et al. [9] first proposed the idea of the operation mode and analyzed five dramatically different operation modes (i.e. translational, rotational, planar (2 types) and mixed motion) of a 3-URU LMPM. Due to the presence of multiple operation modes LMPMs (also named disassembly-free reconfigurable LMPMs, multimode LMPMs or LMPMs with bifurcation of motion), the design of manipulators with multi-functionality can be implemented and has attracted much attention [10-13]. Fanghella et al. [14] proposed several parallel robots with lower-mobility in which the mobile platforms can alter the type of motion when robots are displaced from one operation mode to another. Refaat et al. [15] presented a novel mechanism with two 2-DOF operation modes and used it as a tool head for CNC (Computer Numerical Control) centers. Based on reconfigurable Hooke joints, Gan et al. [16-18] successively presented a series of LMPMs that can switch their operation modes. Kong [19-22] deeply investigated the operation modes of LMPMs. Then a series of multiple operation modes (e.g. spherical translation mode and sphere-on-sphere rolling mode) LMPMs including ones with two DOFs, three DOFs and variable DOFs were presented by type synthesis [19-21]. There is also plenty of research work devoted to the analysis of the operation mode. Significantly, the overall kinematic behavior including operation mode can be explained by analyzing the global kinematics of LMPMs using algebraic geometry [23-28]. For the 3-UPU LMPM, Walter at al. [29] dealt with a complete kinematic analysis by algebraic geometry and presented seven operation modes via a primary decomposition. Stigger et al. [30] analyzed global kinematics of a 3-RUU LMPM with two approaches and two operation modes have been exhibited. As for the three typical 2-DOF pointing mechanisms, the operation modes of them were analyzed to disclose their motion characteristics [31]. Two different operation modes, existing in the typical mechanisms - 3-RPS LMPMs, were presented based on Study parameters [32-34]. In order to exhibit operation modes of LMPMs intuitively, the axodes were applied by means of the velocity operator [35]. According to the above references, it is found that dealing with a prime decomposition of an ideal generated by constraint equations is a critical step to analyze operation modes of

a LMPM. However, for the LMPMs with complicated constraint conditions for which a primary decomposition of the ideal is not feasible, it is difficult to analyze their operation modes. Additionally, motion characteristics of the operation modes are not revealed efficiently and deeply.

This paper aims to provide an efficient and systematical way for analyzing operation modes and revealing corresponding motion characteristics of LMPMs including ones with complicated constraint conditions. Due to the limitation of Euler parameter quaternions and fussy matrix operations of Study parameters, the dual quaternion will be used as an effective tool in this paper. Note that internal collisions and joint limits will not be considered here.

The remainder of this paper is organized as follows: in Section 2, unit dual quaternions are classified into 132 cases with kinematic interpretations based on the number of constant zero components. In Section 3, a general method for analyzing operation modes and reveling corresponding motion characteristics of LMPMs is proposed based on unit dual quaternions. In Section 4, taking a 3-RSR LMPM and a 3-RPS LMPM as examples, their operation modes and axodes are obtained by the proposed approach and motion characteristics are indicated. Finally, conclusions are drawn in Section 5.

2. Classification of unit dual quaternions

A unit dual quaternion [36], which derives from the quaternion and dual number, can be used to describe rotations and translations of a rigid body. In this section, we will first introduce the definition and operation of the dual quaternion.

A dual quaternion is defined as

$$Q = e + \varepsilon g = (e_0 + e_1\mathbf{i} + e_2\mathbf{j} + e_3\mathbf{k}) + \varepsilon(g_0 + g_1\mathbf{i} + g_2\mathbf{j} + g_3\mathbf{k}) \tag{1}$$

where e and g are quaternions that represent real and pure dual quaternion components respectively, ε is a dual operator satisfying $\varepsilon^2=0$ and $\varepsilon\neq 0$.

The product of two dual quaternions satisfies the following rules which are identical to that of two quaternions:

$$\begin{cases} \mathbf{i}^2 = \mathbf{j}^2 = \mathbf{k}^2 = \mathbf{ijk} = -1 \\ \mathbf{ij} = \mathbf{k} = -\mathbf{ji} \\ \mathbf{jk} = \mathbf{i} = -\mathbf{kj} \\ \mathbf{ki} = \mathbf{j} = -\mathbf{ik} \end{cases} \tag{2}$$

There exist three versions of conjugation relations for dual quaternions, Q_a^*, Q_b^* and Q_c^*:

$$\begin{cases} Q_a^* = e^* + \varepsilon g^* = (e_0 - e_1\mathbf{i} - e_2\mathbf{j} - e_3\mathbf{k}) + \varepsilon(g_0 - g_1\mathbf{i} - g_2\mathbf{j} - g_3\mathbf{k}) \\ Q_b^* = e - \varepsilon g = (e_0 + e_1\mathbf{i} + e_2\mathbf{j} + e_3\mathbf{k}) - \varepsilon(g_0 + g_1\mathbf{i} + g_2\mathbf{j} + g_3\mathbf{k}) \\ Q_c^* = e^* - \varepsilon g^* = (e_0 - e_1\mathbf{i} - e_2\mathbf{j} - e_3\mathbf{k}) - \varepsilon(g_0 - g_1\mathbf{i} - g_2\mathbf{j} - g_3\mathbf{k}) \end{cases} \tag{3}$$

where the first version Q_a^* can be used for modeling the motion of lines, while the third version Q_c^* can be adopted to model the motion of points or planes [37].

In addition to the rules aforementioned, for describing poses of a rigid body, the set of unit dual quaternions should be restrained in a manifold satisfying

$$\begin{cases} e_0^2 + e_1^2 + e_2^2 + e_3^2 = 1 \\ e_0 g_0 + e_1 g_1 + e_2 g_2 + e_3 g_3 = 0 \end{cases} \tag{4}$$

Hence, the real dual quaternion component e could denote a rotation around an axis $\boldsymbol{u}$ with an angle θ as

$$e = e_0 + e_1\mathbf{i} + e_2\mathbf{j} + e_3\mathbf{k} = \cos(\theta/2) + \boldsymbol{u}\cdot\sin(\theta/2) \tag{5}$$

Differing from unit quaternions, a unit dual quaternion can represent a translation t of a displacement by

$$\begin{aligned} t &= 2ge^* \\ &= 2(-g_0e_1 + g_1e_0 - g_2e_3 + g_3e_2)\mathbf{i} + 2(-g_0e_2 + g_1e_3 + g_2e_0 - g_3e_1)\mathbf{j} + 2(-g_0e_3 - g_1e_2 + g_2e_1 + g_3e_0)\mathbf{k} \end{aligned} \tag{6}$$

where $2\cdot(-g_0e_1+g_1e_0-g_2e_3+g_3e_2)$, $2\cdot(-g_0e_2+g_1e_3+g_2e_0-g_3e_1)$ and $2\cdot(-g_0e_3-g_1e_2+g_2e_1+g_3e_0)$ denote the translational distance of a rigid body along X-axis, Y-axis, Z-axis respectively.

When a unit dual quaternion is used to represent the pose transformation of a vector $\boldsymbol{r}=\{r_x, r_y, r_z\}^T$, by writing the vector in dual quaternion form as $\boldsymbol{r}=1+\varepsilon(r_x\mathbf{i}+r_y\mathbf{j}+r_z\mathbf{k})$, we have

$${}^a\boldsymbol{r} = Q\boldsymbol{r}Q_c^* \tag{7}$$

where ${}^a\boldsymbol{r}=1+\varepsilon({}^ar_x\mathbf{i}+{}^ar_y\mathbf{j}+{}^ar_z\mathbf{k})$ (or ${}^a\boldsymbol{r}=\{{}^ar_x, {}^ar_y, {}^ar_z\}^T$) stands for a vector obtained from the vector $\boldsymbol{r}$ via pose transformation.

Furthermore, the composite displacement composed of motion Q_1 followed by motion Q_2 with respect to the global and local coordinate system can be represented respectively as follows:

$$\begin{cases} Q = Q_2 Q_1 \\ Q = Q_1 Q_2 \end{cases} \tag{8}$$

Since the parameters (e_0, e_1, e_2, e_3) of a real dual quaternion component e cannot be zero simultaneously and the relationship between e_i and g_i (i=0, 1, 2, 3) fulfills Eq. (4) invariably, unit dual quaternions can be classified into 132 cases on the basis of the number of their constant zero components. It is worth noting that Ref. [22] categorized unit quaternions into 15 cases to describe the operation modes of rotational LMPMs clearly. These 15 cases are expanded to 132 cases using unit dual quaternions here, which can be applied to the analysis of operation modes of LMPMs especially that with both rotational and translational DOFs. Actually, the 132 cases just correspond to the 132 elementary operation modes, and numerous extra operation modes with additional constraint equations can be obtained based on these elementary ones. The kinematic meaning of 8 out of the 132 cases is listed in Table 1. For more information about these cases, see the Appendix.

Table 1 A fraction of the classification of a unit dual quaternion and their kinematic interpretation

No.	Case	Unit dual quaternion	R-DOF	T-DOF	Motion description
14	{0, 0, 0, e_3; g_0, 0, 0, 0}	Q=**k**+εg_0	0	1	Half-turn rotation about the Z-axis and translation along the Z-axis with translational distance 2g_0
61	{e_0, e_1, 0, 0; 0, 0, g_2, g_3}	Q=e_0+e_1**i**+ε(g_2**j**+g_3**k**)	1	2	Rotation by an angle 2atan(e_1, e_0) about the X-axis and translations along the Y-axis and Z-axis with translational distance 2e_0g_2-2e_1g_3 and 2e_0g_3+2e_1g_2 respectively
66	{0, 0, e_2, e_3; g_0, g_1, 0, 0}	Q=e_2**j**+e_3**k**+ε(g_0+g_1**i**)=(e_2+e_3**i**)**j**+ε(g_0+g_1**i**)	1	2	Half-turn rotation about the Y-axis followed by a rotation by an angle 2atan(e_3, e_2) about the X-axis, and translations along the Y-axis and Z-axis with translational distance -2e_2g_0+2e_3g_1 and -2e_2g_1-2e_3g_0 respectively.
79	{e_0, e_1, e_2, 0; 0, 0, 0, g_3}	Q=e_0+e_1**i**+e_2**j**+εg_3**k**=(-e_2**i**+e_1**j**-e_0**k**)**k**+εg_3**k**	2	1	Half-turn rotation about the Z-axis followed by a half-turn rotation about the axis $\boldsymbol{u}$=(-e_2, e_1, -e_0)^T, and translations along the X-axis, Y-axis and Z-axis with translational distance 2e_2g_3, -2e_1g_3 and 2e_0g_3 respectively
115	{0, e_1, e_2, e_3; g_0, g_1, g_2, 0}	Q=e_1**i** +e_2**j**+e_3**k**+ε(g_0+g_1**i**+g_2**j**)	2	2	Half-turn rotation about the axis $\boldsymbol{u}$=(e_1, e_2, e_3)^T and translations along the X-axis, Y-axis and Z-axis with translational distance -2e_1g_0-2e_3g_2, -2e_2g_0+2e_3g_1 and 2e_1g_2-2e_2g_1-2e_3g_0 respectively.
120	{e_0, e_1, e_2, e_3; g_0, 0, 0, g_3}	Q=e_0+e_1**i**+e_2**j**+e_3**k**+ε(g_0+g_3**k**)	3	1	Spherical motion and translations along the X-axis, Y-axis and Z-axis with translational distance -2e_1g_0+2e_2g_3, -2e_1g_3-2e_2g_0 and 2e_0g_3-2e_3g_0 respectively.
121	{e_0, e_1, e_2, e_3; 0, g_1, g_2, 0}	Q=e_0+e_1**i**+e_2**j**+e_3**k**+ε(g_1**i**+g_2**j**)	3	1	Spherical motion and translations along the X-axis, Y-axis and Z-axis with translational distance 2e_0g_1-2e_3g_2, 2e_0g_2+2e_3g_1 and 2e_1g_2-2e_2g_1 respectively.
124	{e_0, e_1, e_2, 0; g_0, g_1, g_2, g_3}	Q=e_0+e_1**i**+e_2**j**+ε(g_0+g_1**i**+g_2**j**+g_3**k**)=(-e_2**i**+e_1**j**-e_0**k**)**k**+ε(g_0+g_1**i**+g_2**j**+g_3**k**)	2	3	Half-turn rotation about the Z-axis followed by a half-turn rotation about the axis $\boldsymbol{u}$=(-e_2, e_1, -e_0)^T, and translations along the X-axis, Y-axis and Z-axis with translational distance 2e_0g_1-2e_1g_0+2e_2g_3, 2e_0g_2-2e_1g_3-2e_2g_0 and 2e_0g_3+2e_1g_2-2e_2g_1 respectively
127	{0, e_1, e_2, e_3; g_0, g_1, g_2, g_3}	Q=e_1**i**+e_2**j**+e_3**k**+ε(g_0+g_1**i**+g_2**j**+g_3**k**)	2	3	Half-turn rotation about the axis $\boldsymbol{u}$=(e_1, e_2, e_3)^T and translations along the X-axis, Y-axis and Z-axis with translational distance -2e_1g_0+2e_2g_3-2e_3g_2, -2e_1g_3-2e_2g_0+2e_3g_1 and 2e_1g_2-2e_2g_1-2e_3g_0 respectively

Note: the numbers listed in Table 1 correspond to that in Appendix so that they are not written in order from 1 to 8.

From Eqs. (5) and (6), the kinematic meaning of 132 cases of the unit dual quaternion can be identified compactly. For instance, the unit dual quaternion of case {0, 0, 0, e_3; g_0, 0, 0, 0} is Q=**k**+εg_0 (No. 14 in Table 1), which denotes a half-turn rotation about the Z-axis and a translation along the Z-axis with translational distance 2g_0. The rotational degree of freedom (R-DOF) of the above motion is zero as illustrated in [22]. In addition, the translational degree of freedom (T-DOF) of the motion is one referring to the number of independent parameters that are not constant in pure dual quaternion components g, and the magnitude of the translation along Z-axis is 2g_0. Moreover, the unit dual quaternion of case {0, e_1, e_2, e_3; g_0, g_1, g_2, 0} is Q=e_1**i** +e_2**j**+e_3**k**+ε(g_0+g_1**i**+g_2**j**) (No. 115 in Table 1), which represents a half-turn rotation about the axis $\boldsymbol{u}$=(e_1, e_2, e_3)^T and translations along the X, Y and Z-axes with translational distance -2e_1g_0-2e_3g_2, -2e_2g_0+2e_3g_1 and 2e_1g_2-2e_2g_1-2e_3g_0 respectively. Transformed into two parts (-2e_1g_0, -2e_2g_0, -2e_3g_0) and (-2e_3g_2, 2e_3g_1, 2e_1g_2-2e_2g_1), the translations can indeed be regarded as components of translation along the axes (-e_1, -e_2, -e_3)^T and (e_1e_3 / ($e_2\sqrt{1+e_1^2/e_2^2}$) , e_3 / $\sqrt{1+e_1^2/e_2^2}$, (-e_1^2 − e_2^2) / ($e_2\sqrt{1+e_1^2/e_2^2}$))^T with translational distance 2g_0 and $2g_1\sqrt{1+e_1^2/e_2^2}$ respectively, which denotes 2 T-DOF. Namely, the DOF of the above motion is four including 2 R-

DOF and 2 T-DOF. The kinematic interpretation of all the 132 cases is provided in Appendix.

3. A general approach for analyzing operation modes and motion characteristics of LMPMs

Operation modes and motion characteristics of LMPMs can be analyzed via the following procedures.

Step 1 Uncover geometrical constraints of the mobile platform and list corresponding constraint equations according to the kinematic structure of a LMPM.

Step 2 Giving an arbitrary pose transformation of the mobile platform, formulate the pose of feature points, lines or planes based on the unit dual quaternion, which reflects the geometrical constraints with respect to the base platform.

Step 3 Upon substituting the coordinates of feature points, lines or planes into the constraint equations obtained in **Step 1**, formulate a polynomial ideal ($I=\langle a_1, a_2, \ldots, a_n\rangle$) generated by constraint equations with parameters e_0, e_1, e_2, e_3, g_0, g_1, g_2 and g_3. The affine varieties determined by the ideal I, which confirm different operation modes of the LMPM, are thus computed by a primary decomposition. In this process, software (e.g. Singular and Maple) can provide effective assistance.

If a polynomial ideal is too complicated that it is not possible to be dealt with a primary decomposition, the process shown in Fig. 1 can be adopted to obtain main operation modes of a LMPM. The details are presented as follows:

Firstly, substitute the 132 cases listed in Appendix into constraint equations in turn to obtain corresponding ideals. Secondly, compute Hilbert Dimension of the affine variety determined by an ideal with Eq. (4). If Hilbert Dimension of the affine variety is greater than 0 that means the mechanism has a corresponding operation mode; otherwise, it corresponding to no operation mode. Then, solve the maximal independent set of the dual quaternion parameters based on the mentioned ideal. The other dual quaternion parameters should be expressed as functions of the maximal independent set. To avoid obtaining repetitive operation modes, all the dual quaternion parameters under the corresponding case should not be vanished identically (note that the constant zero parameters in the corresponding case will not be considered). In addition, if none of the dual quaternion parameters is vanished identically, the corresponding case and its affine variety are recorded. Finally, if all the cases have been considered in turn, the recorded affine varieties that are contained in bigger ones should be eliminated and the main operation modes of a LMPM can be obtained.

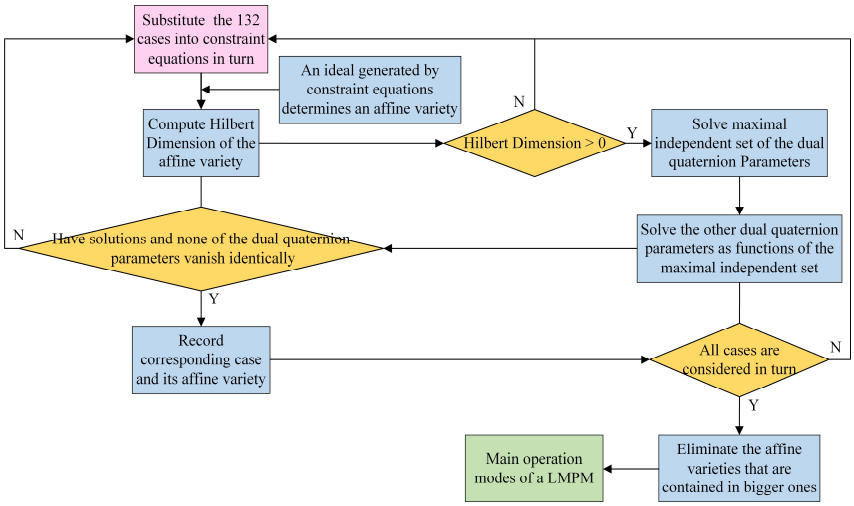

Fig.1 A flowchart of analysis for main operation modes of a LMPM

Step 4 Efficiently obtain the kinematic interpretation of operation modes of a LMPM by referencing the proposed 132 elementary operation modes, such that its motion characteristics are expounded clearly.

Step 5 Draw the axodes to gain a deeper insight into the physical meaning of the operation modes and motion characteristics.

An axode is a surface formed by the path of a series of instantaneous screw axes (ISAs). Essentially, a screw motion about an ISA can represent the general motion of a spatial mechanism. In the next section, the proposed procedures will be illustrated by examples with 2R1T DOF.

Mechanism and Machine Theory, 2019, Vol 142, 103577
https://doi.org/10.1016/j.mechmachtheory.2019.103577

4. Examples of operation mode analysis

4.1 Operation mode analysis of the 3-RSR LMPM

A 2R1T DOF 3-RSR LMPM, shown in Fig. 1, is one of the zero-torsion mechanisms composed of a mobile platform connected to the base by three identical RSR limbs. Each limb is a serial kinematic chain composed of rotational (R), spherical (S) and R joints in sequence and the distances between the S joint to the two R joints are equal. This LMPM has been extensively used in numerous fields. Nevertheless, its operation mode is not revealed fully. In this section, the operation mode analysis of the 3-RSR LMPM will be treated below to better understand the mechanism.

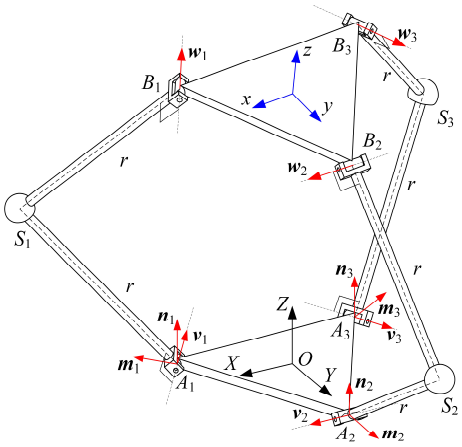

Fig. 2. Schematic of a 3-RSR LMPM

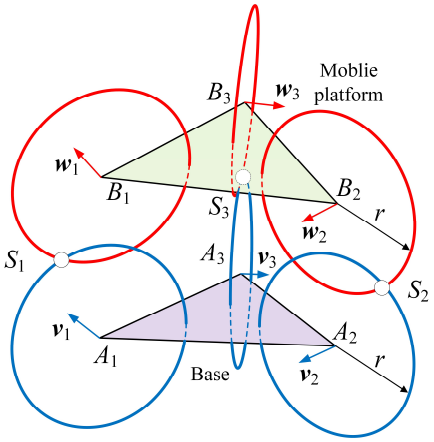

Fig. 3. Constraint model of a 3-RSR LMPM

With reference to Fig. 2, S_i (i=1, 2, 3) is the center of the spherical joint. A_i (i=1, 2, 3) and B_i (i=1, 2, 3) are the feet of the perpendicular through S_i to the axes of the rotational joints fixed to the base and the mobile platform respectively. Simultaneously, A_i and B_i are the vertices of the base and mobile platform which are consisted of the equilateral triangle. r is the length of the connecting rods S_iA_i and S_iB_i. $\boldsymbol{w}_i$ (i=1, 2, 3) and $\boldsymbol{v}_i$ (i=1, 2, 3) are the unit vectors of the R joint axes fixed to the mobile platform and the base respectively. $\boldsymbol{m}_i$ (i=1, 2, 3) and $\boldsymbol{n}_i$ (i=1, 2, 3) are two mutually orthogonal unit vectors that are perpendicular to $\boldsymbol{v}_i$ and fixed to the base. O-XYZ is the global coordinate system whose origin coincides with the center of the base. The Y-axis passes through A_2 and the Z-axis is perpendicular to the base. The X-axis is defined by the Y- and Z-axes by mean of the right-hand rule. o-xyz is the local coordinate system fixed to the mobile platform, whose layout is completely analog. Again, the origin coincides with the center of the mobile platform. The y-axis passes through B_2 and the z-axis is perpendicular to the mobile platform. The x-axis is determined by the y- and z-axis using the right-hand rule as well.

Since the point S_i must lie both on the circumference perpendicular to $\boldsymbol{v}_i$ with center A_i and radius r, and on another circumference perpendicular to $\boldsymbol{w}_i$ with center B_i and radius r [38] as demonstrated in Fig. 3, the geometrical conditions of the 3-RSR LMPM can be written as

$$\begin{cases} (\boldsymbol{S}_i - \boldsymbol{A}_i)^2 = r^2 \\ (\boldsymbol{S}_i - \boldsymbol{B}_i)^2 = r^2 \\ (\boldsymbol{S}_i - \boldsymbol{A}_i)\cdot \boldsymbol{v}_i = 0 \\ (\boldsymbol{S}_i - \boldsymbol{B}_i)\cdot \boldsymbol{w}_i = 0 \end{cases} \quad i=1,\ 2 \text{ and } 3 \tag{9}$$

where $\boldsymbol{S}_i$, $\boldsymbol{A}_i$ and $\boldsymbol{B}_i$ are the position vectors of points S_i, A_i and B_i respectively. $\boldsymbol{S}_i$ can be expressed as

$$\boldsymbol{S}_i = y_i\boldsymbol{m}_i + z_i\boldsymbol{n}_i \tag{10}$$

where y_i (i=1, 2, 3) and z_i (i=1, 2, 3) are coefficients. The substitution of Eq. (10) into Eq. (9) gives

$$y_i^2 + z_i^2 + \boldsymbol{A}_i^2 - 2y_i(\boldsymbol{m}_i\cdot\boldsymbol{A}_i) - 2z_i(\boldsymbol{n}_i\cdot\boldsymbol{A}_i) - r^2 = 0 \tag{11a}$$

$$y_i^2 + z_i^2 + \boldsymbol{B}_i^2 - 2y_i(\boldsymbol{m}_i\cdot\boldsymbol{B}_i) - 2z_i(\boldsymbol{n}_i\cdot\boldsymbol{B}_i) - r^2 = 0 \tag{11b}$$

$$y_i(\boldsymbol{m}_i\cdot\boldsymbol{v}_i) + z_i(\boldsymbol{n}_i\cdot\boldsymbol{v}_i) - \boldsymbol{A}_i\cdot\boldsymbol{v}_i = 0 \tag{11c}$$

$$y_i(\boldsymbol{m}_i\cdot\boldsymbol{w}_i) + z_i(\boldsymbol{n}_i\cdot\boldsymbol{w}_i) - \boldsymbol{B}_i\cdot\boldsymbol{w}_i = 0 \tag{11d}$$

Then substituting Eq. (11a) into Eq. (11b) and removing the identical equation Eq. (11c), the geometrical conditions are rewritten as follows

$$y_i^2 + z_i^2 + \boldsymbol{B}_i^2 - 2y_i(\boldsymbol{m}_i \cdot \boldsymbol{B}_i) - 2z_i(\boldsymbol{n}_i \cdot \boldsymbol{B}_i) - r^2 = 0 \tag{12a}$$

$$2y_i\left[\boldsymbol{m}_i \cdot (\boldsymbol{A}_i - \boldsymbol{B}_i)\right] + 2z_i\left[\boldsymbol{n}_i \cdot (\boldsymbol{A}_i - \boldsymbol{B}_i)\right] - \boldsymbol{A}_i^2 + \boldsymbol{B}_i^2 = 0 \tag{12b}$$

$$y_i(\boldsymbol{m}_i \cdot \boldsymbol{w}_i) + z_i(\boldsymbol{n}_i \cdot \boldsymbol{w}_i) - \boldsymbol{B}_i \cdot \boldsymbol{w}_i = 0 \tag{12c}$$

From Eqs. (12b) and (12c), the explicit expressions of y_i and z_i can be derived as

$$\begin{cases} y_i = \dfrac{a_i}{c_i} \\ z_i = \dfrac{b_i}{c_i} \end{cases} \tag{13}$$

where

$$\begin{cases} a_i = 0.5(\boldsymbol{A}_i^2 - \boldsymbol{B}_i^2)(\boldsymbol{n}_i \cdot \boldsymbol{w}_i) - (\boldsymbol{B}_i \cdot \boldsymbol{w}_i)\left[\boldsymbol{n}_i \cdot (\boldsymbol{A}_i - \boldsymbol{B}_i)\right] \\ b_i = -0.5(\boldsymbol{A}_i^2 - \boldsymbol{B}_i^2)(\boldsymbol{m}_i \cdot \boldsymbol{w}_i) + (\boldsymbol{B}_i \cdot \boldsymbol{w}_i)\left[\boldsymbol{m}_i \cdot (\boldsymbol{A}_i - \boldsymbol{B}_i)\right] \\ c_i = (\boldsymbol{n}_i \cdot \boldsymbol{w}_i)\left[\boldsymbol{m}_i \cdot (\boldsymbol{A}_i - \boldsymbol{B}_i)\right] - (\boldsymbol{m}_i \cdot \boldsymbol{w}_i)\left[\boldsymbol{n}_i \cdot (\boldsymbol{A}_i - \boldsymbol{B}_i)\right] \end{cases}$$

Upon substitution of Eq. (13) into Eq. (12a), the constraint equations can be obtained as follows

$$a_i^2 + b_i^2 - 2a_ic_i\boldsymbol{m}_i \cdot \boldsymbol{B}_i - 2b_ic_i\boldsymbol{n}_i \cdot \boldsymbol{B}_i - c_i^2(r_i^2 - \boldsymbol{B}_i^2) = 0 \tag{14}$$

According to Fig. 2, the geometric constants of the 3-RSR LMPM are assigned to be

$$\boldsymbol{A}_1 = \left[\sqrt{3}/2,\ -1/2,\ 0\right]^{\mathrm{T}},\ \boldsymbol{A}_2 = \left[0,\ 1,\ 0\right]^{\mathrm{T}},\ \boldsymbol{A}_3 = \left[-\sqrt{3}/2,\ -1/2,\ 0\right]^{\mathrm{T}},\ \boldsymbol{v}_1 = \left[-1/2,\ -\sqrt{3}/2,\ 0\right]^{\mathrm{T}},$$

$$\boldsymbol{v}_2 = \left[1,\ 0,\ 0\right]^{\mathrm{T}},\ \boldsymbol{v}_3 = \left[-1/2,\ \sqrt{3}/2,\ 0\right]^{\mathrm{T}},\ \boldsymbol{m}_1 = \left[\sqrt{3}/2,\ -1/2,\ 0\right]^{\mathrm{T}},\ \boldsymbol{m}_2 = \left[0,\ 1,\ 0\right]^{\mathrm{T}},$$

$$\boldsymbol{m}_3 = \left[-\sqrt{3}/2,\ -1/2,\ 0\right]^{\mathrm{T}},\ \boldsymbol{n}_1 = \left[0,\ 0,\ 1\right]^{\mathrm{T}},\ \boldsymbol{n}_2 = \left[0,\ 0,\ 1\right]^{\mathrm{T}},\ \boldsymbol{n}_3 = \left[0,\ 0,\ 1\right]^{\mathrm{T}} \text{ and } r = 2.$$

Once the pose of the mobile platform transforms arbitrarily (giving arbitrary rotations and translations), in terms of Eq. (7), $\boldsymbol{B}_i$ and $\boldsymbol{w}_i$ attaching to the mobile platform in the global coordinate system can be computed

$$\begin{cases} \boldsymbol{B}_i = Q\boldsymbol{B}_{oi}Q_c^* \\ \boldsymbol{w}_i = Q\boldsymbol{w}_{oi}Q_c^* \end{cases} i = 1,\ 2 \text{ and } 3 \tag{15}$$

where $\boldsymbol{B}_{o1} = [\sqrt{3}/2,\ -1/2,\ 0]^{\mathrm{T}}$, $\boldsymbol{B}_{o2} = [0,\ 1,\ 0]^{\mathrm{T}}$, $\boldsymbol{B}_{o3} = [-\sqrt{3}/2,\ -1/2,\ 0]^{\mathrm{T}}$, $\boldsymbol{w}_{o1} = [-1/2,\ -\sqrt{3}/2,\ 0]^{\mathrm{T}}$, $\boldsymbol{w}_{o2} = [1,\ 0,\ 0]^{\mathrm{T}}$ and $\boldsymbol{w}_{o3} = [-1/2,\ \sqrt{3}/2,\ 0]^{\mathrm{T}}$, which are measured in local coordinate system. It turns out that

$$\begin{cases} \boldsymbol{B}_1 = 1 + \varepsilon\left(\begin{array}{l} (\frac{\sqrt{3}}{2}e_0^2 + \frac{\sqrt{3}}{2}e_1^2 - \frac{\sqrt{3}}{2}e_2^2 - \frac{\sqrt{3}}{2}e_3^2 + e_0e_3 - e_1e_2 - 2e_3g_2 - 2e_1g_0 + 2e_2g_3 + 2e_0g_1)\mathbf{i} + \\ (-\frac{1}{2}e_0^2 + \frac{1}{2}e_1^2 - \frac{1}{2}e_2^2 + \frac{1}{2}e_3^2 + \sqrt{3}e_0e_3 + \sqrt{3}e_1e_2 + 2e_0g_2 - 2e_1g_3 - 2e_2g_0 + 2e_3g_1)\mathbf{j} + \\ (\sqrt{3}e_1e_2 - \sqrt{3}e_0e_2 - e_2e_3 - e_0e_1 + 2e_0g_3 + 2e_1g_2 - 2e_2g_1 - 2e_3g_0)\mathbf{k} \end{array}\right) \\ \boldsymbol{B}_2 = 1 + \varepsilon\left[\begin{array}{l} (2e_0g_1 - 2e_1g_0 + 2e_2g_3 - 2e_3g_2 + 2e_1e_2 - 2e_0e_3)\mathbf{i} + \\ (2e_0g_2 - 2e_1g_3 - 2e_2g_0 + 2e_3g_1 + e_0^2 - e_1^2 + e_2^2 - e_3^2)\mathbf{j} \\ +(2e_0g_3 + 2e_1g_2 - 2e_2g_1 - 2e_3g_0 + 2e_0e_1 + 2e_2e_3)\mathbf{k} \end{array}\right] \\ \boldsymbol{B}_3 = 1 + \varepsilon\left(\begin{array}{l} (-\frac{\sqrt{3}}{2}e_0^2 - \frac{\sqrt{3}}{2}e_1^2 + \frac{\sqrt{3}}{2}e_2^2 + \frac{\sqrt{3}}{2}e_3^2 + e_0e_3 - e_1e_2 + 2e_0g_1 - 2e_1g_0 + 2e_2g_3 - 2e_3g_2)\mathbf{i} + \\ (-\frac{1}{2}e_0^2 + \frac{1}{2}e_1^2 - \frac{1}{2}e_2^2 + \frac{1}{2}e_3^2 - \sqrt{3}e_0e_3 - \sqrt{3}e_1e_2 + 2e_0g_2 - 2e_1g_3 - 2e_2g_0 + 2e_3g_1)\mathbf{j} + \\ (\sqrt{3}e_0e_2 - \sqrt{3}e_1e_3 - e_2e_3 - e_0e_1 + 2e_0g_3 + 2e_1g_2 - 2e_2g_1 - 2e_3g_0)\mathbf{k} \end{array}\right) \end{cases} \tag{16}$$

$$\begin{cases} \boldsymbol{w}_1 = 1+\varepsilon\left[\begin{array}{l}\left(\frac{1}{2}e_0^2+\frac{1}{2}e_1^2-\frac{1}{2}e_2^2-\frac{1}{2}e_3^2-\sqrt{3}e_0e_3+\sqrt{3}e_1e_2\right)\mathbf{i}+\\ \left(\frac{\sqrt{3}}{2}e_0^2-\frac{\sqrt{3}}{2}e_1^2+\frac{\sqrt{3}}{2}e_2^2-\frac{\sqrt{3}}{2}e_3^2+e_0e_3+e_1e_2\right)\mathbf{j}+\\ \left(e_1e_3-e_0e_2+\sqrt{3}e_0e_1+\sqrt{3}e_2e_3\right)\mathbf{k}\end{array}\right] \\ \boldsymbol{w}_2 = 1+\varepsilon\left[\left(e_0^2+e_1^2-e_2^2-e_3^2\right)\mathbf{i}+\left(2e_0e_3+2e_1e_2\right)\mathbf{j}+\left(-2e_0e_2+2e_1e_3\right)\mathbf{k}\right] \\ \boldsymbol{w}_3 = 1+\varepsilon\left[\begin{array}{l}\left(-\frac{1}{2}e_0^2-\frac{1}{2}e_1^2+\frac{1}{2}e_2^2+\frac{1}{2}e_3^2-\sqrt{3}e_0e_3+\sqrt{3}e_1e_2\right)\mathbf{i}+\\ \left(\frac{\sqrt{3}}{2}e_0^2-\frac{\sqrt{3}}{2}e_1^2+\frac{\sqrt{3}}{2}e_2^2-\frac{\sqrt{3}}{2}e_3^2-e_0e_3-e_1e_2\right)\mathbf{j}\\ +\left(-e_1e_3+e_0e_2+\sqrt{3}e_0e_1+\sqrt{3}e_2e_3\right)\mathbf{k}\end{array}\right] \end{cases} \tag{17}$$

Substituting these parameters into Eq. (14), the constraint equations with e_0, e_1, e_2, e_3, g_0, g_1, g_2 and g_3 are obtained after some elementary manipulations

$$\begin{cases} \mathrm{a}_1 : -3e_1^2e_3^2-2e_1^2e_3g_1+e_1^2g_0^2+e_1^2g_1^2-8e_1e_2e_3g_2 \\ -6e_1e_3^2g_3-4e_1e_3g_1g_3+2e_1g_0^2g_3+2e_1g_1^2g_3 \\ -4e_2^2g_2^2-8e_2e_3g_2g_3+e_3^2g_2^2-3e_3^2g_3^2-2e_3g_1g_2^2 \\ -2e_3g_1g_3^2+g_0^2g_2^2+g_0^2g_3^2+g_1^2g_2^2+g_1^2g_3^2=0 \\ \mathrm{a}_2 : -12e_1^2e_3^2+52e_1^2e_3g_1+4e_1^2g_0^2-35e_1^2g_1^2-9e_1^2g_2^2-8e_1e_2e_3g_2-36e_1e_2g_1g_2+48e_1^2e_3g_3 \\ -112e_1e_2g_1g_3-16e_1g_0^2g_3-4e_1g_1^2g_3-12e_1g_2^2g_3-36e_2^2e_3^2-36e_2^2e_3g_1+12e_2^2g_0^2-9e_2^2g_1^2 \\ +5e_2^2g_2^2-80e_2e_3g_2g_3-24e_2g_1g_2g_3+12e_3^2g_1^2+4e_3^2g_2^2-48e_3^2g_3^2+12e_3g_1^3-20e_3g_1g_2^2 \\ +16e_3g_1g_3^2+12g_0^2g_1^2+4g_0^2g_2^2+16g_0^2g_3^2+3g_1^4-2g_1^2g_2^2+4g_1^2g_3^2+3g_2^4+12g_2^2g_3^2=0 \\ \mathrm{a}_3 : 6e_1^2e_3g_2-13e_1^2g_1g_2+12e_1e_2e_3^2-20e_1e_2e_3g_1-4e_1e_2g_0^2-13e_1e_2g_1^2-7e_1e_2g_2^2-8e_1e_3g_2g_3 \\ +4e_1g_1g_2g_3-14e_2^2e_3g_2-7e_2^2g_1g_2-24e_2e_3^2g_3-8e_2e_3g_1g_3+8e_2g_0^2g_3+2e_2g_1^2g_3 \\ +6e_2g_2^2g_3+4e_3^2g_1g_2-2e_3g_1^2g_2-2e_3g_2^2-8e_3g_2g_3^2+4g_0^2g_1g_2-2g_1^3g_2+2g_1g_2^2-4g_1g_2g_3^2=0 \end{cases} \tag{18}$$

As a matter of fact, it is not possible to deal with a primary decomposition of the ideal $I=\langle \mathrm{a}_1, \mathrm{a}_2, \mathrm{a}_3\rangle$ generated by the three constraint equations in Eq. (18).

Then the specific process proposed in Section 3 is adopted to obtained main operation modes of the 3-RSR LMPM. It is found that seven operation modes matching with the 3-RSR LMPM are acquired as explicitly listed in Table 2, including two elementary operation modes and five extra operation modes that are deduced from elementary operation modes. The listed operation modes are more complete than that presented in [39]. It is worth noting that internal collisions and joint limits are not considered when these operation modes are obtained. In addition, the mentioned process also can not obtain all the operation modes of the 3-RSR LMPM and there may have 1- or 2-DOF operation modes that are not listed in Table 2.

Table 2 Operation modes of the 3-RSR LMPM

Item	Case	Type	R-DOF	T-DOF	Motion Description	Remarks
l_1	{0, 0, 0, e_3; g_0, 0, 0, 0}	elementary operation modes	0	1	Half-turn rotation about the Z-axis and translation along the Z-axis with translational distance $2g_0$	None
l_2	{e_0, e_1, e_2, 0; 0, 0, 0, g_3}		2	1	Half-turn rotation about the Z-axis followed by a half-turn rotation about the axis $\boldsymbol{u}$=(-e_2, e_1, -e_0)^T, and translations along the X-axis, Y-axis and Z-axis with translational distance $2e_2g_3$, $-2e_1g_3$ and $2e_0g_3$ respectively.	None
l_3	{e_0, e_1, 0, 0; 0, 0, g_2, g_3}	Extra operation modes	1	1	Rotation by an angle 2atan(e_1, e_0) about the X-axis and translations along the Y-axis and Z-axis with translational distance $2e_0g_2$-$2e_1g_3$ and $2e_0g_3$+$2e_1g_2$ respectively	$g_3=\frac{1}{2}\sqrt{1-e_0^2}-\frac{1}{2}\sqrt{4-4e_0^2-g_2^2}$

l_4	$\{0, 0, e_2, e_3; g_0, g_1, 0, 0\}$	1	1	Half-turn rotation about the Y-axis followed by a rotation by an angle $2\text{atan}(e_3, e_2)$ about the X-axis, and translations along the Y-axis and Z-axis with translational distance $-2e_2g_0+2e_3g_1$ and $-2e_2g_1-2e_3g_0$ respectively.	$g_0=\sqrt{-\frac{-12e_2^2g_1\sqrt{1-e_2^2}+4g_1^3\sqrt{1-e_2^2}+12e_2^4-7e_2^2g_1^2+g_1^4-12e_2^2+4g_1^2}{4e_2^2+4g_1^2}}$
l_5	$\{0, e_1, e_2, e_3; g_0, g_1, g_2, 0\}$	1	1	Half-turn rotation about the axis $\boldsymbol{u}=(e_1, e_2, e_3)^T$ and translations along the X-axis, Y-axis and Z-axis with translational distance $-2e_1g_0-2e_3g_2$, $-2e_2g_0+2e_3g_1$ and $2e_1g_2-2e_2g_1-2e_3g_0$ respectively.	$e_2=-\frac{\sqrt{3}}{3}e_1$, $e_3=\sqrt{-\frac{4}{3}e_1^2+1}$, $g_1=\frac{\sqrt{3}}{3}g_2$, $g_0=\sqrt{-\frac{6\sqrt{3}g_2\sqrt{9-12e_1^2}-2\sqrt{3}g_2^3\sqrt{9-12e_1^2}+36e_1^4-21e_1^2g_2^2+3g_2^4-27e_1^2+9g_2^2}{9e_1^2+9g_2^2}}$
l_6	$\{e_0, e_1, e_2, e_3; g_0, 0, 0, g_3\}$	3	0	Spherical motion and translations along the X-axis, Y-axis and Z-axis with translational distance $-2e_1g_0+2e_2g_3$, $-2e_1g_3-2e_2g_0$ and $2e_0g_3-2e_3g_0$ respectively.	$g_0=-\sqrt{3}e_3$, $g_3=\sqrt{3}e_0$
l_7	$\{e_0, e_1, e_2, e_3; 0, g_1, g_2, 0\}$	3	0	Spherical motion and translations along the X-axis, Y-axis and Z-axis with translational distance $2e_0g_1-2e_3g_2$, $2e_0g_2+2e_3g_1$ and $2e_1g_2-2e_2g_1$ respectively.	$g_1=-\sqrt{3}e_2$, $g_2=\sqrt{3}e_1$

Note: $e_0g_0+e_1g_1+e_2g_2+e_3g_3=0$, $e_0^2+e_1^2+e_2^2+e_3^2=1$.

Configurations under the operation modes l_1~l_7 are shown in Fig. 4(a)~4(g) respectively. It should be noted that, in some operation modes (such as l_1, l_4, l_5, l_6 and l_7), the 3-RSR LMPM no longer has a zero-torsion characteristic. Additionally, due to space limitations, only the operation modes l_2 which the 3-RSR LMPM always hold will be discussed in detail, while other operation modes of the 3-RSR LMPM will not be explored here.

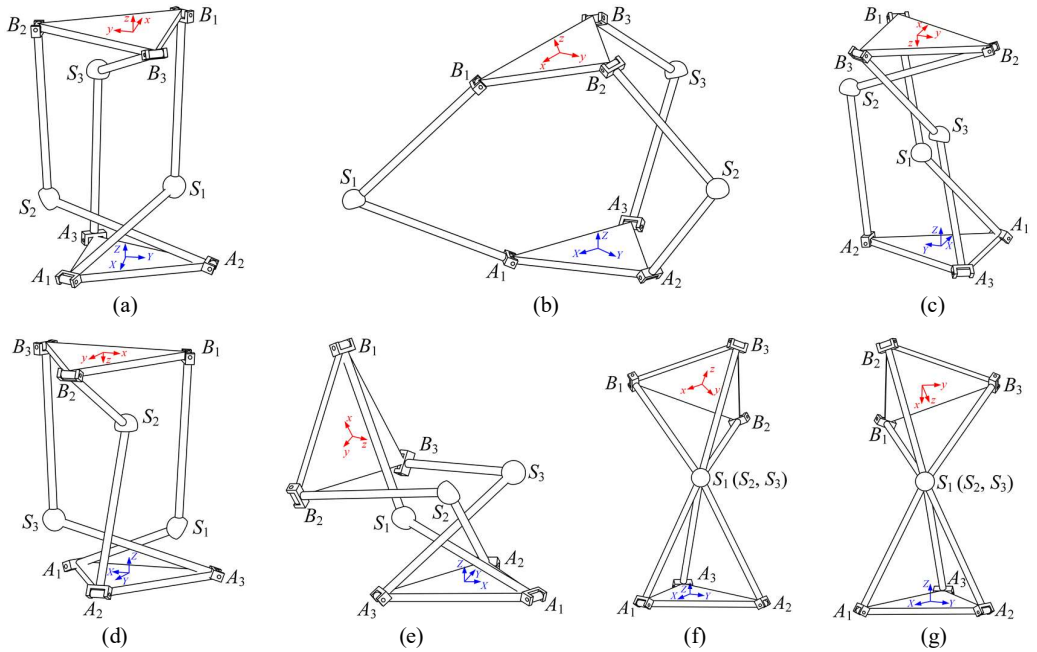

Fig.4. Configurations in different operation modes of the 3-RSR LMPM, (a) is in operation mode l_1, (b) is in operation mode l_2, (c) is in operation mode l_3, (d) is in operation mode l_4, (e) is in operation mode l_5, (f) is in operation mode l_6, (g) is in operation mode l_7

4.2 Axodes of the 3-RSR LMPM under the Operation Mode l_2

In order to get a deeper insight into the physical meaning of the operation modes and motion characteristics, axodes are analyzed and drawn as follows. There are three main methods (e.g. Jacobian matrix method [40], graphical approach [41] and velocity operator [42]) used to solve the ISAs and axodes. In fact, a graphical approach is the graphical representation of a Jacobian matrix method and the theoretical basis of both methods is screw theory. Nevertheless, the graphical approach is only suitable for the mechanisms having obvious geometrical constraint

characteristics, and the Jacobian matrix method is too complicated that both the inverse and forward Jacobian matrix have to be analyzed. Naturally, the velocity operator, which is related to the pose transformation, is adopted to solve the axodes in this paper.

From the entries of the velocity operator [42], the ISAs of the motion of the mobile platform are obtained by means of unit dual quaternions

$$\begin{aligned} \boldsymbol{ISA} &= \dot{Q}Q_{\mathrm{a}}^{*} = \left[(\dot{e}_0+\dot{e}_1\mathbf{i}+\dot{e}_2\mathbf{j}+\dot{e}_3\mathbf{k})+\varepsilon(\dot{g}_0+\dot{g}_1\mathbf{i}+\dot{g}_2\mathbf{j}+\dot{g}_3\mathbf{k})\right]\left[(e_0-e_1\mathbf{i}-e_2\mathbf{j}-e_3\mathbf{k})+\varepsilon(g_0-g_1\mathbf{i}-g_2\mathbf{j}-g_3\mathbf{k})\right] \\ &= (s_1\mathbf{i}+s_2\mathbf{j}+s_3\mathbf{k})+\varepsilon(s_1\mathbf{i}+s_2\mathbf{j}+s_3\mathbf{k}) \end{aligned} \tag{19}$$

where

$$\begin{aligned} s_1 &= -\dot{e}_0e_1+\dot{e}_1e_0-\dot{e}_2e_3+\dot{e}_3e_2\,,\quad s_2 = -\dot{e}_0e_2+\dot{e}_1e_3+\dot{e}_2e_0-\dot{e}_3e_1\,,\quad s_3 = -\dot{e}_0e_3-\dot{e}_1e_2+\dot{e}_2e_1+\dot{e}_3e_0\,, \\ s_4 &= -\dot{e}_0g_1+\dot{e}_1g_0-\dot{e}_2g_3+\dot{e}_3g_2-\dot{g}_0e_1+\dot{g}_1e_0-\dot{g}_2e_3+\dot{g}_3e_2\,, \\ s_5 &= -\dot{e}_0g_2+\dot{e}_1g_3+\dot{e}_2g_0-\dot{e}_3g_1-\dot{g}_0e_2+\dot{g}_1e_3+\dot{g}_2e_0-\dot{g}_3e_1\,, \\ s_6 &= -\dot{e}_0g_3-\dot{e}_1g_2+\dot{e}_2g_1+\dot{e}_3g_0-\dot{g}_0e_3-\dot{g}_1e_2+\dot{g}_2e_1+\dot{g}_3e_0\,. \end{aligned}$$

The corresponding Plücker coordinates of the ISA are given by [43]

$$\boldsymbol{ISA} = (s_1,\ \ s_2,\ \ s_3;\ \ s_4,\ \ s_5,\ \ s_6) \tag{20}$$

According to the analysis in the previous subsection, the transformation of the mobile platform under the operation mode l_2 can be written as

$$Q = (e_0+e_1\mathbf{i}+e_2\mathbf{j})+\varepsilon(g_3\mathbf{k}) \tag{21}$$

Thus, the ISA is given by

$$\boldsymbol{ISA} = \left((-\dot{e}_0e_1+\dot{e}_1e_0)\mathbf{i}+(-\dot{e}_0e_2+\dot{e}_2e_0)\mathbf{j}+(-\dot{e}_1e_2+\dot{e}_2e_1)\mathbf{k}\right)+\varepsilon\left((-\dot{e}_2g_3+\dot{g}_3e_2)\mathbf{i}+(\dot{e}_1g_3-\dot{g}_3e_1)\mathbf{j}+(-\dot{e}_0g_3+\dot{g}_3e_0)\mathbf{k}\right) \tag{22}$$

Since the axodes of mechanisms with multi-DOF have various possibilities, the corresponding axodes analysis will only allow one parameter to determine the pose. To draw the axodes of the 3-RSR LMPM as a simple example, the parameters are chosen to be e_0=cos(t/2), e_1=0, e_2=sin(t/2), g_3=1+t. Under this assumption, the fixed ISA is reduced to

$$\boldsymbol{ISA}_{\mathrm{F}} = \left(\frac{1}{2}\mathbf{j}\right)+\varepsilon\left((\sin\frac{t}{2}-\frac{1}{2}(1+t)\cos\frac{t}{2})\mathbf{i}+(\cos\frac{t}{2}+\frac{1}{2}(1+t)\sin\frac{t}{2})\mathbf{k}\right)$$

As a result, the fixed ISAs of the mobile platform in Plücker coordinates can be acquired by normalization:

$$\boldsymbol{ISA}_{\mathrm{F}} = \left(0\quad 1\quad 0;\quad 2\sin\frac{t}{2}-(1+t)\cos\frac{t}{2}\quad 0\quad 2\cos\frac{t}{2}+(1+t)\sin\frac{t}{2}\right)$$

On the other hand, according to the inversion of the 3-RSR LMPM, the moving ISAs of the mobile platform are obtained as follows

$$\boldsymbol{ISA}_{\mathrm{M}} = \left(0\quad 1\quad 0;\quad (1+t)\cos\frac{t}{2}-2\sin\frac{t}{2}-2\quad 0\quad 2\cos\frac{t}{2}+(1+t)\sin\frac{t}{2}\right)$$

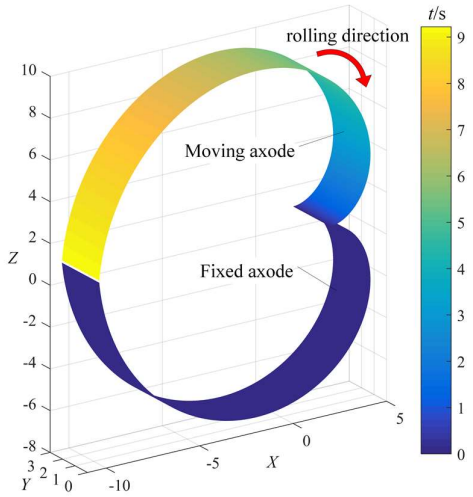

Fig. 5. Axodes when e_0=cos(t/2), e_1=0, e_2=sin(t/2) and g_3=1+t

Mechanism and Machine Theory, 2019, Vol 142, 103577
https://doi.org/10.1016/j.mechmachtheory.2019.103577

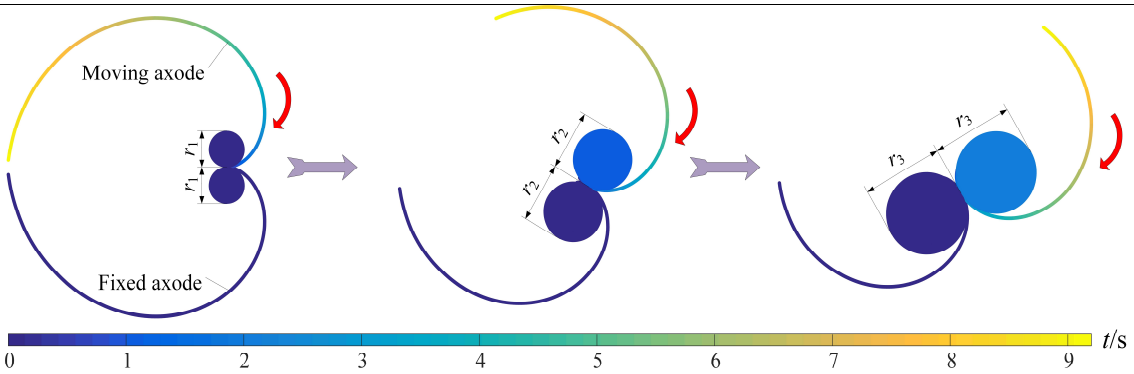

Fig. 6. Movement process of the moving axode rolling on the fixed axode

When t varies from 0 to 2.94π, a series of twists corresponding to the ISAs at every instant are obtained as shown in Fig. 5. The purple surface denotes the fixed axode computed with respect to the fixed coordinate system, while the polychrome surface indicates the moving axode relating to the mobile platform. The colour bar represents the time when a moving ISA coincides with a corresponding fixed ISA, which also suggests the kinematic velocity of the platform. Based on Poinsot theorem, the movement of the mobile platform in this case can be considered as the moving axode rolls on the fixed axode along the direction without sliding, as illustrated in Fig. 6.

Fig. 6 demonstrates the movement of the moving axode with respect to the fixed one. It can be regarded as a pure rolling (without sliding) between two identical cylindrical surfaces at any moment, with the cylinder diameter changing over time. As shown in Fig. 6, the diameter of the cylinder increases gradually satisfying $r_1 \neq r_2 \neq r_3$.

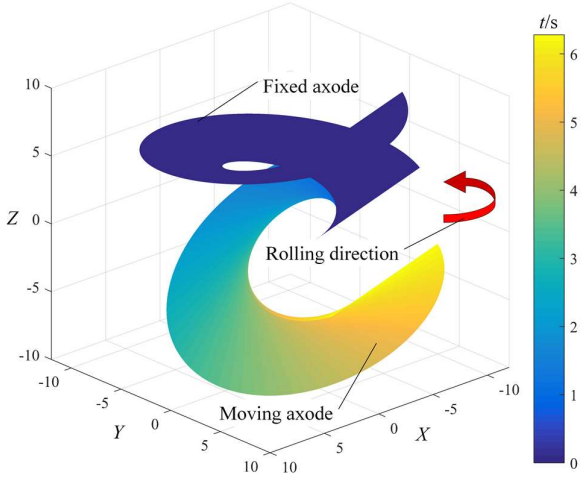

Fig. 7. Axodes when e_0=cos(π/12), e_1=-sin(t)sin(π/12), e_2=cos(t)sin(π/12) and g_3=1+t

In the same vein, when choosing e_0=cos(π/12), e_1=-sin(t)sin(π/12), e_2=cos(t)sin(π/12) and g_3=1+t, the fixed and moving ISAs can be derived as

$$\begin{cases} \boldsymbol{ISA}_{\mathrm{F}} = \left(s_{11} \quad s_{12} \quad s_{13};\ s_{14} \quad s_{15} \quad s_{16}\right) \\ \boldsymbol{ISA}_{\mathrm{M}} = \left(s_{21} \quad s_{22} \quad s_{23};\ s_{24} \quad s_{24} \quad s_{26}\right) \end{cases} \tag{23}$$

where

$$s_{11} = -\frac{1}{2}\cos t\,,\quad s_{12} = -\frac{1}{2}\sin t\,,\quad s_{13} = 1-\frac{\sqrt{3}}{2}\,,\quad s_{14} = (\frac{\sqrt{6}-\sqrt{2}}{2}+\frac{\sqrt{6}-\sqrt{2}}{2}t)\sin t+\frac{\sqrt{6}-\sqrt{2}}{2}\cos t\,,$$

$$s_{15} = -(\frac{\sqrt{6}-\sqrt{2}}{2}+\frac{\sqrt{6}-\sqrt{2}}{2}t)\cos t+\frac{\sqrt{6}-\sqrt{2}}{2}\sin t\,,\quad s_{16} = \frac{\sqrt{6}+\sqrt{2}}{2}\,,\quad s_{21} = 5\sqrt{3}\cos t+10-5\sqrt{3}\,,\quad s_{22} = 10\sin t\,,$$

$$s_{23} = -5\cos t + 10\sqrt{3} - 15\,,\; s_{24} = (10\sqrt{2} - 10\sqrt{6} + (15\sqrt{2} - 5\sqrt{6})t)\sin t + (15\sqrt{2} - 5\sqrt{6})\cos t - 5(\sqrt{6} + \sqrt{2})\,,$$

$$s_{25} = ((15\sqrt{2} - 5\sqrt{6}) + (10\sqrt{2} - 10\sqrt{6})t)\cos t + (10\sqrt{6} - 10\sqrt{2})\sin t + (15\sqrt{6} - 25\sqrt{2})\,,$$

$$s_{26} = ((5\sqrt{2} - 5\sqrt{6})t)\sin t + (5\sqrt{2} - 5\sqrt{6})\cos t - (15\sqrt{2} + 5\sqrt{6})\,.$$

The corresponding axodes are drawn in Fig. 7. It is apparent that the fixed axode and the moving axode are a pair of helicoidal surfaces. The movement of the mobile platform in this condition can be viewed as a helicoidal axode rolls on the same fixed one without sliding.

To consider the above both two motions simultaneously, the instantaneous velocity centers of the mobile platform compose a nautilicone surface shown in Fig. 8, when assigning e_0=cos(t/2), e_1=-sin(t)sin(t/2), e_2=cos(t)sin(t/2) and g_3=1+t. It can be concluded that the movement of the mobile platform is equivalent to a pure rolling between two identical nautilicone surfaces. Due to the presence of one T-DOF in the 3-RSR LMPM, the mechanism can realize an equal-diameter spherical pure rolling with variable diameters as kinematic characteristics, and it has a great potential to be used as a special transmission.

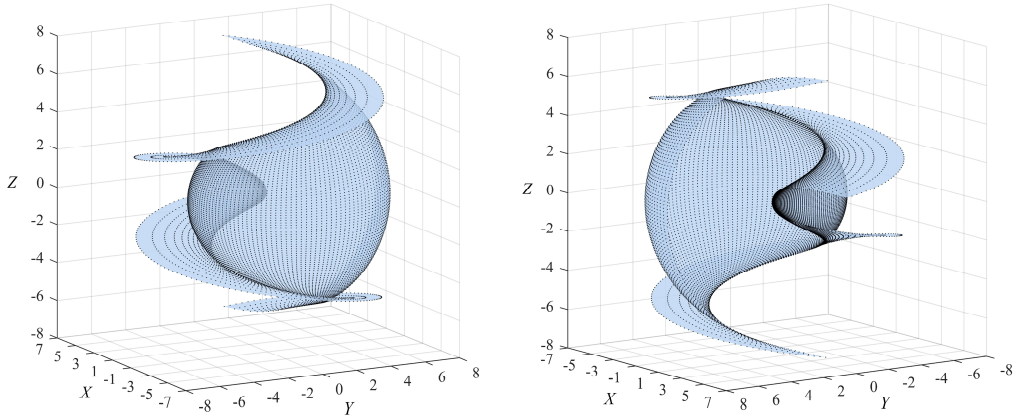

Fig. 8. A curved surface composed of instantaneous velocity centers of the mobile platform

Note that the kinematic characteristics of the 3-RSR LMPM shown in Figs. 5-8 are arisen under the condition that the translational distance of the mobile platform changes as g_3=1+t along the direction of T-DOF. For different parameters in the operation mode, the movement of the mobile platform will be altered to some extent and various axodes can be obtained, whereas the kinematic characteristics of the mechanism will not be changed.

4.3 Operation mode analysis of the 3-RPS LMPM

The 3-RPS LMPM [44] as shown in Fig. 9 is one of the most popular LMPMs consisting of a base, a mobile platform and three identical RPS limbs, where the rotational and spherical joints in each limb are attached to the base and the mobile platform respectively. The operation modes of this mechanism have been solved using Study parameters in Ref. [32]. Nevertheless, the axodes and motion characteristics in the operation modes have not been discussed comprehensively. In this section, the operation mode analysis of the 3-RPS LMPM will be addressed based on the unit dual quaternion to better comprehend the mechanism.

Mechanism and Machine Theory, 2019, Vol 142, 103577
https://doi.org/10.1016/j.mechmachtheory.2019.103577

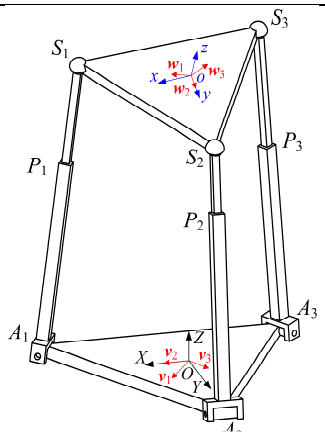

Fig. 9. Schematic of the 3-RPS LMPM

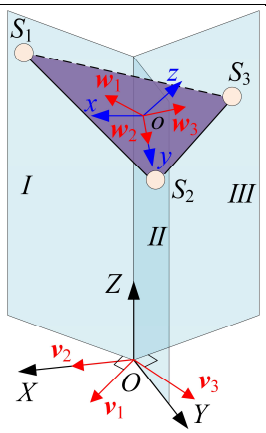

Fig. 10. Constraint model of the 3-RPS LMPM

Since the motion direction of the prismatic joint is perpendicular to the axis of the rotational joint for each limb, the three spherical joints are restricted to move in the vertical planes (plane *I*, plane *II*, plane *III* in Fig.10) intersecting at a common line at 120º angles. Hence, the geometrical constraints can be obtained as [34]

$$\boldsymbol{w}_i \cdot \boldsymbol{v}_i = 0\ ,\ i=1,\ 2,\ 3 \tag{24}$$

where $\boldsymbol{v}_1$, $\boldsymbol{v}_2$ and $\boldsymbol{v}_3$ are the unit vectors perpendicular to the plane *I*, *II* and *III* respectively, $\boldsymbol{w}_i$ is the unit vector along oS_i (i=1, 2, 3). Their coordinates with respect to the global coordinate system can be denoted as

$$\begin{cases} \boldsymbol{v}_1 = 1+\varepsilon\left(\dfrac{1}{2}\mathbf{i}+\dfrac{\sqrt{3}}{2}\mathbf{j}\right) \\ \boldsymbol{v}_2 = 1+\varepsilon(\mathbf{i}) \\ \boldsymbol{v}_3 = 1+\varepsilon\left(-\dfrac{1}{2}\mathbf{i}+\dfrac{\sqrt{3}}{2}\mathbf{j}\right) \end{cases} \tag{25}$$

$$\begin{cases} \boldsymbol{w}_1 = 1+\varepsilon\left[\begin{array}{l}(\frac{\sqrt{3}}{2}e_0^2+\frac{\sqrt{3}}{2}e_1^2-\frac{\sqrt{3}}{2}e_2^2-\frac{\sqrt{3}}{2}e_3^2+e_0e_3-e_1e_2-2e_3g_2-2e_1g_0+2e_2g_3+2e_0g_1)\mathbf{i}+\\ (-\frac{1}{2}e_0^2+\frac{1}{2}e_1^2-\frac{1}{2}e_2^2+\frac{1}{2}e_3^2+\sqrt{3}e_0e_3+\sqrt{3}e_1e_2+2e_0g_2-2e_1g_3-2e_2g_0+2e_3g_1)\mathbf{j}+\\ (\sqrt{3}e_1e_2-\sqrt{3}e_0e_2-e_2e_3-e_0e_1+2e_0g_3+2e_1g_2-2e_2g_1-2e_3g_0)\mathbf{k}\end{array}\right] \\ \boldsymbol{w}_2 = 1+\varepsilon\left[\begin{array}{l}(2e_0g_1-2e_1g_0+2e_2g_3-2e_3g_2+2e_1e_2-2e_0e_3)\mathbf{i}+\\ (2e_0g_2-2e_1g_3-2e_2g_0+2e_3g_1+e_0^2-e_1^2+e_2^2-e_3^2)\mathbf{j}\\ +(2e_0g_3+2e_1g_2-2e_2g_1-2e_3g_0+2e_0e_1+2e_2e_3)\mathbf{k}\end{array}\right] \\ \boldsymbol{w}_3 = 1+\varepsilon\left[\begin{array}{l}(-\frac{\sqrt{3}}{2}e_0^2-\frac{\sqrt{3}}{2}e_1^2+\frac{\sqrt{3}}{2}e_2^2+\frac{\sqrt{3}}{2}e_3^2+e_0e_3-e_1e_2+2e_0g_1-2e_1g_0+2e_2g_3-2e_3g_2)\mathbf{i}+\\ (-\frac{1}{2}e_0^2+\frac{1}{2}e_1^2-\frac{1}{2}e_2^2+\frac{1}{2}e_3^2-\sqrt{3}e_0e_3-\sqrt{3}e_1e_2+2e_0g_2-2e_1g_3-2e_2g_0+2e_3g_1)\mathbf{j}+\\ (\sqrt{3}e_0e_2-\sqrt{3}e_1e_3-e_2e_3-e_0e_1+2e_0g_3+2e_1g_2-2e_2g_1-2e_3g_0)\mathbf{k}\end{array}\right] \end{cases} \tag{26}$$

By substituting Eqs. (25) and (26) into Eq. (24), one obtains

$$\begin{cases} \mathrm{a}_1 : 2e_0e_3+e_1e_2+e_0g_1-e_1g_0+e_2g_3-e_3g_2=0 \\ \mathrm{a}_2 : e_1e_2-e_0e_3+e_0g_1-e_1g_0+e_2g_3-e_3g_2=0 \\ \mathrm{a}_3 : e_1^2-e_2^2+e_0g_2-e_1g_3-e_2g_0+e_3g_1=0 \end{cases} \tag{27}$$

Fortunately, the primary decomposition of the ideal $I=\langle \mathrm{a}_1, \mathrm{a}_2, \mathrm{a}_3\rangle$ generated by Eq. (27) can be acquired via Singular as follows:

$$I = \bigcap_{j=1}^{2} I_j \tag{28}$$

where

$$l_1 = \langle e_0,\ e_1e_2 - e_1g_0 - e_3g_2 + e_2g_3,\ e_1^2 - e_2^2 - 2e_2g_0 + 2e_3g_1 - 2e_1g_3 \rangle$$
$$l_2 = \langle e_3,\ e_1e_2 - e_1g_0 + e_0g_1 + e_2g_3,\ e_1^2 - e_2^2 - 2e_2g_0 + 2e_0g_2 - 2e_1g_3 \rangle$$

It is certain that the 3-RPS LMPM has two different operation modes as listed in Table 3, which do not belong to the 132 elementary operation modes but can be derived from that. For the first operation mode l_1. Substituting g_0, g_1 and g_3 into the expressions of translations in Table 3 yields translational distance along *X*-axis, *Y*-axis, and *Z*-axis by $-2e_1e_2$, $-e_1^2+e_2^2$ and $(2g_2-2e_1e_2e_3)/e_1$ respectively. It is worth to note that the translations along the *X*-axis and *Y*-axis are only determined by the orientation parameters (e.g. e_0, e_1 and e_2), which are called parasitic motion as an important characteristic of the mechanism mentioned in Ref. [45]. Namely, the T-DOF of the 3-RPS LMPM is one and its direction is along the *Z*-axis. Moreover, in this operation mode, the mobile platform can not achieve the target pose from the home pose via pure translations, because e_0=0 and e_1, e_2, e_3 can not be equal to zero in this condition simultaneously. This means that a rotation with an angle π consequentially exists in the transformation of the pose. For the second operation mode l_2, translations of the mechanism along the *X*-axis, *Y*-axis and *Z*-axis can be expressed as $-2e_1e_2$, $-e_1^2+e_2^2$ and $(-2g_1-2e_0e_1e_2)/e_2$ respectively, which are similar to that within the first operation mode. Nevertheless, the character of rotations between the two operation modes is different. Additionally, the configurations under the two modes are shown in Fig. 11. In what follows, the axodes of both operation modes will be given.

Table 3 Operation modes of the 3-RPS LMPM

Item	Case	Type	R-DOF	T-DOF	Motion Description	Remarks
l_1	$\{0, e_1, e_2, e_3; g_0, g_1, g_2, g_3\}$	Extra operation modes	2	1	Half-turn rotation about the axis $\boldsymbol{u}=(e_1, e_2, e_3)^T$ and translations along the *X*-axis, *Y*-axis and *Z*-axis with translational distance $-2e_1g_0 + 2e_2g_3 - 2e_3g_2$, $-2e_1g_3 - 2e_2g_0 + 2e_3g_1$ and $2e_1g_2 - 2e_2g_1 - 2e_3g_0$ respectively.	$g_0=\frac{1}{2}(e_1^2e_2 - 3e_2^3 + 2e_2 - \frac{2e_3g_2}{e_1})$, $g_1=-\frac{1}{2}(e_1^2e_3 - 3e_2^2e_3 + \frac{2e_2g_2}{e_1})$, $g_3=\frac{1}{2}(e_1^3 - 3e_1e_2^2)$
l_2	$\{e_0, e_1, e_2, 0; g_0, g_1, g_2, g_3\}$		2	1	Half-turn rotation about the *Z*-axis followed by a half-turn rotation about the axis $\boldsymbol{u}=(-e_2,\ e_1,\ -e_0)^T$, and translations along the *X*-axis, *Y*-axis and *Z*-axis with translational distance $2e_0g_1 - 2e_1g_0 + 2e_2g_3$, $2e_0g_2 - 2e_1g_3 - 2e_2g_0$ and $2e_0g_3 + 2e_1g_2 - 2e_2g_1$ respectively.	$g_0=\frac{1}{2}e_2(3e_1^2 - e_2^2)$, $g_2=-\frac{1}{2}(e_0^3 + 4e_0e_1^2 - e_0 + \frac{2e_1g_1}{e_2})$, $g_3=\frac{1}{2}(e_1(e_0^2 + 4e_1^2 - 3) - \frac{2e_0g_1}{e_2})$

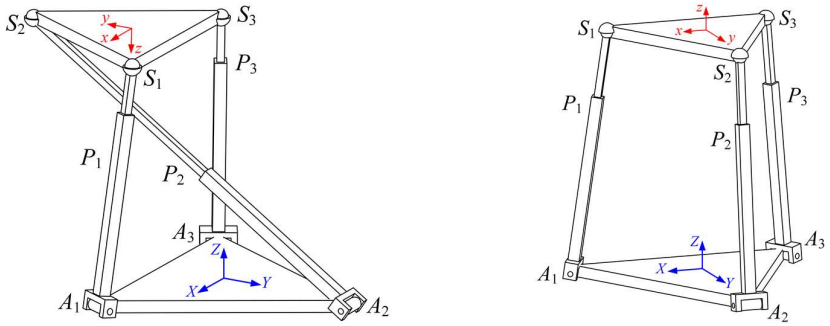

(a) (b)

Fig. 11 Configurations in different operation modes of the 3-RPS LMPM, (a) is in operation mode l_1, (b) is in operation mode l_2

4.4 Analysis of axodes of the 3-RPS LMPM under the Operation Modes

4.4.1 Axodes analysis under the first Operation Mode

In the first operation mode of the 3-RPS LMPM, the pose transformation of the mobile platform in dual quaternion form can be written as

Mechanism and Machine Theory, 2019, Vol 142, 103577
https://doi.org/10.1016/j.mechmachtheory.2019.103577

$$Q=(e_1\mathbf{i}+e_2\mathbf{j}+e_3\mathbf{k})+\varepsilon\left(\frac{1}{2}(e_1^2e_2-3e_2^3+2e_2-\frac{2e_3g_2}{e_1})-\frac{1}{2}(e_1^2e_3-3e_2^2e_3+\frac{2e_2g_2}{e_1})\mathbf{i}+(g_2)\mathbf{j}+\frac{1}{2}(e_1^3-3e_1e_2^2)\mathbf{k}\right) \quad (29)$$

To draw the axodes of the 3-RPS LMPM，one can assign e_1=cos(t)sin(π/12), e_2=sin(t)sin(π/12), e_3=cos(π/12), g_2=((t+1)e_1+2$e_1e_2e_3$)/2. As a result, the fixed ISA can be expressed as

$$\boldsymbol{ISA}_{\mathrm{F}}=(s_{11}\quad s_{12}\quad s_{13};\ s_{14}\quad s_{15}\quad s_{16})$$

where

$$s_{11}=-\frac{1}{2}\cos(t),\quad s_{12}=-\frac{1}{2}\sin(t),\quad s_{13}=1-\frac{\sqrt{3}}{2},\quad s_{14}=\frac{1}{2}(1+t)\sin(t)+\left(2\sqrt{3}-\frac{15}{4}\right)\cos^2(t)-\sqrt{3}+\frac{15}{8},$$

$$s_{15}=\left(\frac{15}{4}-2\sqrt{3}\right)\sin(t)\cos(t)-\frac{1}{2}(1+t)\cos(t),\quad s_{16}=\left(\frac{\sqrt{3}}{2}-1\right)\cos^3(\mathrm{t})+\left(\frac{3}{4}-\frac{3\sqrt{3}}{8}\right)\cos(\mathrm{t})+1.$$

In this case, the Plücker coordinates $\boldsymbol{ISA}_{\mathrm{M}}$=($s_{21}$, s_{22}, s_{23}; s_{24}, s_{25}, s_{26}) of the moving ISA can be expressed by

$$s_{21}=-\frac{\sqrt{3}}{4}\cos(t)+\frac{\sqrt{3}-2}{4},\quad s_{22}=-\frac{1}{2}\sin(t),\quad s_{23}=\frac{1}{4}\cos(t)+\frac{3-2\sqrt{3}}{4},$$

$$s_{24}=\left(\frac{7\sqrt{3}}{2}-6\right)\cos^4(t)+\left(\frac{\sqrt{3}}{2}-1\right)\cos^3(t)+\left(6-\frac{29\sqrt{3}}{8}\right)\cos^2(t)+\left(\frac{5}{8}-\frac{9\sqrt{3}}{16}\right)\cos(t)+\frac{1}{2}\sin(t)+\frac{19\sqrt{3}-24}{16},$$

$$s_{25}=\left(7-4\sqrt{3}\right)\sin(t)\cos^3(t)+\left(2\sqrt{3}-\frac{13}{4}\right)\sin(t)\cos(t)-\frac{\sqrt{3}}{4}\cos(t)-\frac{1}{2}\sin(t)+\frac{\sqrt{3}-2}{4},$$

$$s_{26}=\left(2\sqrt{3}-\frac{7}{2}\right)\cos^4(t)+\left(\frac{3}{2}-\sqrt{3}\right)\cos^3(t)+\left(\frac{29}{8}-2\sqrt{3}\right)\cos^2(t)+\left(\frac{5\sqrt{3}}{8}-\frac{11}{16}\right)\cos(t)+\frac{8\sqrt{3}-3}{16}.$$

Furthermore, solving the pitch of $\boldsymbol{ISA}_{\mathrm{M}}$, we obtain

$$h_2=\frac{s_{21}s_{24}+s_{22}s_{25}+s_{23}s_{26}}{s_{21}^2+s_{22}^2+s_{23}^2}=\cos^3(t)-\frac{3}{4}\cos(t)+\frac{1}{2} \quad (30)$$

Eq. (30) means that the mobile platform has sliding motion along the ISA during the process of the rolling, which is caused by parasitic motions.

When t varies from 0 to 2π, the corresponding axodes are plotted in Fig. 12. It is obvious that the fixed and moving axodes are helicoid-like and cone-like ruled surfaces separately different from those in Fig. 7. The sliding line represents the space trajectory of a point on the moving ISA, which reflects the sliding of the mobile platform during the rolling.

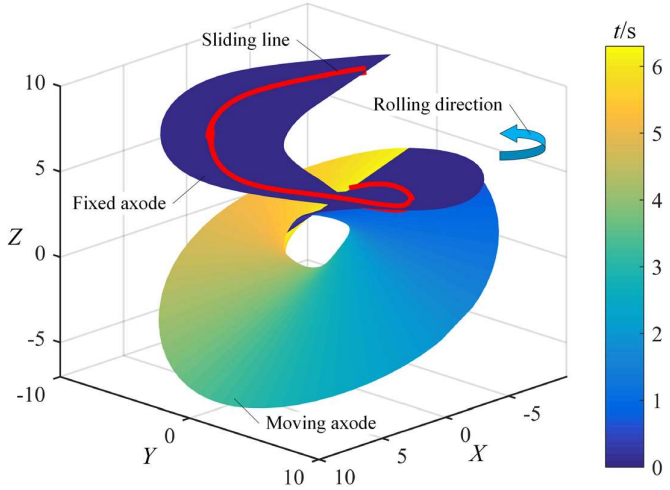

Fig. 12. Axodes of 3-RPS LMPM when e_1=cos(t)sin(π/12), e_2=sin(t)sin(π/12), e_3=cos(π/12), g_2=((t+1)e_1+2$e_1e_2e_3$)/2

Analogously, when e_1= sin(t/2), e_2=0, e_3=cos(t/2), g_2=((t+1)e_1)/2, the fixed and moving ISAs can be given as

$$\begin{cases} \boldsymbol{ISA}_{\mathrm{F}} = \left(0 \;\; 1 \;\; 0; \;\; -1-t \;\; -\frac{1}{2}\sin(t) \;\; 1\right) \\ \boldsymbol{ISA}_{\mathrm{M}} = \left(0 \;\; 1 \;\; 0; \;\; -1-\sin(t) \;\; -\frac{1}{2}\sin(t) \;\; \cos(t)\right) \end{cases} \tag{31}$$

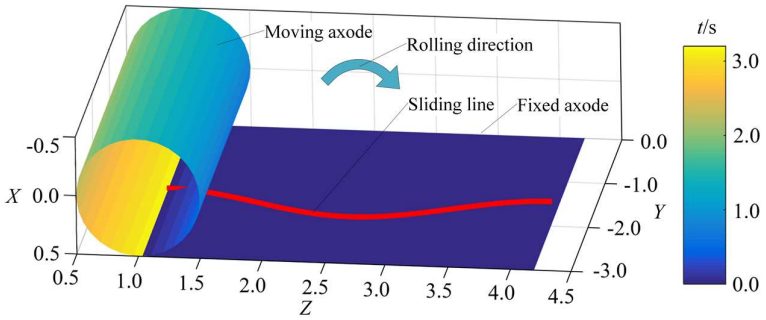

Fig. 13. Axodes of 3-RPS LMPM when e_1= sin(t/2), e_2=0, e_3=cos(t/2), g_2=((t+1)e_1)/2

Fig. 13 displays the motion of the mobile platform in this case: a cylindrical surface rolls on a plane with sliding along the ISAs.

The above analysis shows that, when the orientation of the 3-RPS LMPM changes continuously in the first operation mode, the motion of the mobile platform can be regarded as a rolling movement with sliding along the ISA.

4.4.2 Axodes analysis under the second Operation Mode

In the same manner, the axodes of the 3-RPS LMPM under the second operation mode l_2 can be drawn as shown in Figs. 14 and 15 corresponding to the conditions e_0=cos(π/12), e_1=-sin(t)sin(π/12), e_2=cos(t)sin(π/12), g_2=-(((t+1)e_2+2$e_0e_1e_2$)/2 and e_0=cos(t/2), e_1=0, e_2= sin(t/2), g_2=-((t+1)e_2)/2.

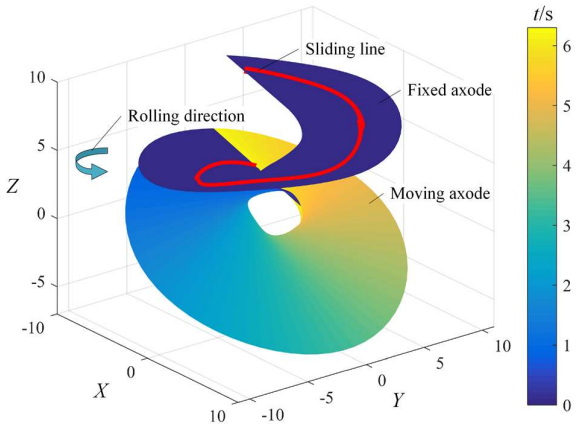

Fig. 14. Axodes of 3-RPS LMPM when e_0=cos(π/12), e_1=-sin(t)sin(π/12), e_2=cos(t)sin(π/12), g_2=-(((t+1)e_2+2$e_0e_1e_2$)/2

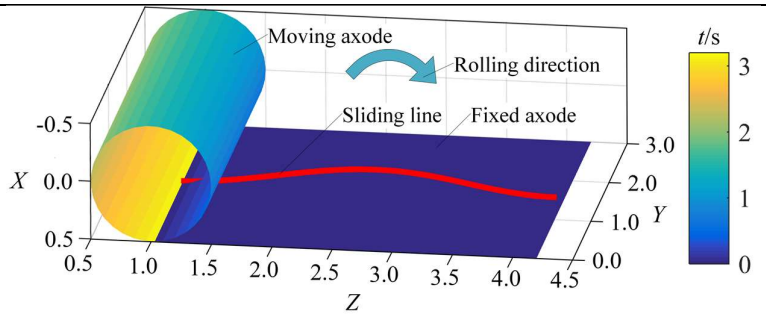

Fig. 15. Axodes of 3-RPS LMPM when $e_0=\cos(t/2)$, $e_1=0$, $e_2=\sin(t/2)$, $g_2=-((t+1)e_2)/2$

There are some similarities between the two operation modes as reflected in the axodes. From the axodes, one can also find that the motion characteristics of the two operation modes are distinct.

5. Conclusions and future research

The unit dual quaternion has been categorized into 132 cases corresponding to the 132 elementary operation modes. The kinematic interpretation of all the cases of unit dual quaternions has been presented in detail. Based on these results, a general method has been presented for analyzing operation modes and revealing corresponding motion characteristics of LMPMs with five steps: (a) uncover geometrical constraints of the mobile platform and list constraint equations according to the kinematic structure of a LMPM; (b) based on the dual quaternion, formulate the pose of feature points, lines or planes reflecting the geometrical constraints with respect to the base platform; (c) substitute coordinates of feature points, lines or planes into constraint equations, and then formulate a polynomial ideal. The affine varieties determined by the ideal are solved by choosing different approaches according to whether the ideal can be dealt with a primary decomposition; (d) obtain the kinematic interpretation of the operation modes of a LMPM efficiently by referencing the proposed 132 elementary operation modes; and (e) draw the axodes by velocity operator in dual quaternion representations. The analysis demonstrates that the 3-RSR LMPM has two elementary operation modes and five extra operation modes. Under the operation mode that the 3-RSR LMPM always holds, it can realize an equal-diameter spherical pure rotation with variable diameters. Therefore, it can be used potentially as a gear pair with variable standard pitch diameters. Moreover, the 3-RSR LMPM has been proved that it can even not exhibits zero-torsion characteristic under certain operation modes. The 3-RSR LMPM is worth to be further researched in future work due to its complicated constraint equations. As for the 3-RPS LMPM, it has two different operation modes in which rolling movements accompanied by sliding along the ISA can be achieved. It is of interest to exhibit the motion characteristics of LMPMs by the rolling that has high movement efficiency.

Furthermore, the classification and kinematic interpretation of the unit dual quaternion presented in this paper can also be extended to analyze operation modes and corresponding motion characteristics of other LMPMs regardless of their DOFs, and plenty of extra operation modes can be derived based on the 132 elementary operation modes.

Acknowledgment

The authors gratefully acknowledge the financial support of the NSFC (Grant No. 51575017).

Appendix

Table I The classification of a unit dual quaternion and their kinematic interpretation

No.	Case	Unit Dual Quaternion	R-DOF	T-DOF	Motion Description
1	$\{e_0, 0, 0, 0; 0, 0, 0, 0\}$	$Q=1$	0	0	No motion
2	$\{0, e_1, 0, 0; 0, 0, 0, 0\}$	$Q=\mathbf{i}$			Half-turn rotation about the X-axis
3	$\{0, 0, e_2, 0; 0, 0, 0, 0\}$	$Q=\mathbf{j}$			Half-turn rotation about the Y-axis
4	$\{0, 0, 0, e_3; 0, 0, 0, 0\}$	$Q=\mathbf{k}$			Half-turn rotation about the Z-axis

5	$\{e_0, 0, 0, 0; 0, g_1, 0, 0\}$	$Q=1+\varepsilon(g_1\mathbf{i})$			Translation along the X-axis with translational distance $2g_1$
6	$\{e_0, 0, 0, 0; 0, 0, g_2, 0\}$	$Q=1+\varepsilon(g_2\mathbf{j})$			Translation along the Y-axis with translational distance $2g_2$
7	$\{e_0, 0, 0, 0; 0, 0, 0, g_3\}$	$Q=1+\varepsilon(g_3\mathbf{k})$			Translation along the Z-axis with translational distance $2g_3$
8	$\{0, e_1, 0, 0; g_0, 0, 0, 0\}$	$Q=\mathbf{i}+\varepsilon(g_0)$			Half-turn rotation about the X-axis and translation along the X-axis with translational distance $-2g_0$
9	$\{0, e_1, 0, 0; 0, 0, g_2, 0\}$	$Q=\mathbf{i}+\varepsilon(g_2\mathbf{j})$			Half-turn rotation about the X-axis and translation along the Z-axis with translational distance $2g_2$
10	$\{0, e_1, 0, 0; 0, 0, 0, g_3\}$	$Q=\mathbf{i}+\varepsilon(g_3\mathbf{k})$			Half-turn rotation about the X-axis and translation along the Y-axis with translational distance $-2g_3$
11	$\{0, 0, e_2, 0; g_0, 0, 0, 0\}$	$Q=\mathbf{j}+\varepsilon(g_0)$	0	1	Half-turn rotation about the Y-axis and translation along the Y-axis with translational distance $-2g_0$
12	$\{0, 0, e_2, 0; 0, g_1, 0, 0\}$	$Q=\mathbf{j}+\varepsilon(g_1\mathbf{i})$			Half-turn rotation about the Y-axis and translation along the Z-axis with translational distance $-2g_1$
13	$\{0, 0, e_2, 0; 0, 0, 0, g_3\}$	$Q=\mathbf{j}+\varepsilon(g_3\mathbf{k})$			Half-turn rotation about the Y-axis and translation along the X-axis with translational distance $2g_3$
14	$\{0, 0, 0, e_3; g_0, 0, 0, 0\}$	$Q=\mathbf{k}+\varepsilon(g_0)$			Half-turn rotation about the Z-axis and translation along the Z-axis with translational distance $2g_0$
15	$\{0, 0, 0, e_3; 0, g_1, 0, 0\}$	$Q=\mathbf{k}+\varepsilon(g_1\mathbf{i})$			Half-turn rotation about the Z-axis and translation along the Y-axis with translational distance $2g_1$
16	$\{0, 0, 0, e_3; 0, 0, g_2, 0\}$	$Q=\mathbf{k}+\varepsilon(g_2\mathbf{j})$			Half-turn rotation about the Z-axis and translation along the X-axis with translational distance $-2g_2$
17	$\{e_0, e_1, 0, 0; 0, 0, 0, 0\}$	$Q=e_0+e_1\mathbf{i}$			Rotation by an angle $2\text{atan}(e_1, e_0)$ about the X-axis
18	$\{e_0, 0, e_2, 0; 0, 0, 0, 0\}$	$Q=e_0+e_2\mathbf{j}$			Rotation by an angle $2\text{atan}(e_2, e_0)$ about the Y-axis
19	$\{e_0, 0, 0, e_3; 0, 0, 0, 0\}$	$Q=e_0+e_3\mathbf{k}$			Rotation by an angle $2\text{atan}(e_3, e_0)$ about the Z-axis
20	$\{0, e_1, e_2, 0; 0, 0, 0, 0\}$	$Q=e_1\mathbf{i}+e_2\mathbf{j}=(e_1+e_2\mathbf{k})\mathbf{i}=(e_2-e_1\mathbf{k})\mathbf{j}$	1	0	Half-turn rotation about the X-axis followed by a rotation by an angle $2\text{atan}(e_2, e_1)$ about Z-axis.
21	$\{0, e_1, 0, e_3; 0, 0, 0, 0\}$	$Q=e_1\mathbf{i}+e_3\mathbf{k}=(e_1-e_3\mathbf{j})\mathbf{i}=(e_3+e_1\mathbf{j})\mathbf{k}$			Half-turn rotation about the X-axis followed by a rotation by an angle $2\text{atan}(-e_3, e_1)$ about the Y-axis or half-turn rotation about the Z-axis followed by a rotation by an angle $2\text{atan}(e_1, e_3)$ about the Y-axis
22	$\{0, 0, e_2, e_3; 0, 0, 0, 0\}$	$Q=e_2\mathbf{j}+e_3\mathbf{k}=(e_2+e_3\mathbf{i})\mathbf{j}=(e_3-e_2\mathbf{i})\mathbf{k}$			Half-turn rotation about the Y-axis followed by a rotation by an angle $2\text{atan}(e_3, e_2)$ about the X-axis or half-turn rotation about the Z-axis followed by a rotation by an angle $2\text{atan}(e_3, -e_2)$ about the X-axis
23	$\{e_0, 0, 0, 0; 0, g_1, g_2, 0\}$	$Q=1+\varepsilon(g_1\mathbf{i}+g_2\mathbf{j})$			Translations along the X-axis and Y-axis with translational distance $2g_1$ and $2g_2$ respectively
24	$\{e_0, 0, 0, 0; 0, g_1, 0, g_3\}$	$Q=1+\varepsilon(g_1\mathbf{i}+g_3\mathbf{j})$			Translations along the X-axis and Z-axis with translational distance $2g_1$ and $2g_3$ respectively
25	$\{e_0, 0, 0, 0; 0, 0, g_2, g_3\}$	$Q=1+\varepsilon(g_2\mathbf{j}+g_3\mathbf{k})$			Translations along the Y-axis and Z-axis with translational distance $2g_2$ and $2g_3$ respectively
26	$\{0, e_1, 0, 0; g_0, 0, g_2, 0\}$	$Q=\mathbf{i}+\varepsilon(g_0+g_2\mathbf{j})$			Half-turn rotation about the X-axis and translations along the X-axis and Z-axis with translational distance $-2g_0$ and $2g_2$ respectively
27	$\{0, e_1, 0, 0; g_0, 0, 0, g_3\}$	$Q=\mathbf{i}+\varepsilon(g_0+g_3\mathbf{k})$			Half-turn rotation about the X-axis and translations along the X-axis and Y-axis with translational distance $-2g_0$ and $-2g_3$ respectively
28	$\{0, e_1, 0, 0; 0, 0, g_2, g_3\}$	$Q=\mathbf{i}+\varepsilon(g_2\mathbf{j}+g_3\mathbf{k})$			Half-turn rotation about the X-axis and translations along the Y-axis and Z-axis with translational distance $-2g_3$ and $2g_2$ respectively
29	$\{0, 0, e_2, 0; g_0, g_1, 0, 0\}$	$Q=\mathbf{j}+\varepsilon(g_0+g_1\mathbf{i})$	0	2	Half-turn rotation about the Y-axis and translations along the Y-axis and Z-axis with translational distance $-2g_0$ and $-2g_1$ respectively
30	$\{0, 0, e_2, 0; g_0, 0, 0, g_3\}$	$Q=\mathbf{j}+\varepsilon(g_0+g_3\mathbf{k})$			Half-turn rotation about the Y-axis and translations along the X-axis and Y-axis with translational distance $2g_3$ and $-2g_0$ respectively
31	$\{0, 0, e_2, 0; 0, g_1, 0, g_3\}$	$Q=\mathbf{j}+\varepsilon(g_1\mathbf{i}+g_3\mathbf{k})$			Half-turn rotation about the Y-axis and translations along the X-axis and Z-axis with translational distance $2g_3$ and $-2g_1$ respectively
32	$\{0, 0, 0, e_3; g_0, g_1, 0, 0\}$	$Q=\mathbf{k}+\varepsilon(g_0+g_1\mathbf{i})$			Half-turn rotation about the Z-axis and translations along the Y-axis and Z-axis with translational distance $2g_1$ and $-2g_0$ respectively
33	$\{0, 0, 0, e_3; g_0, 0, g_2, 0\}$	$Q=\mathbf{k}+\varepsilon(g_0+g_2\mathbf{j})$			Half-turn rotation about the Z-axis and translations along the X-axis and Z-axis with translational distance $-2g_2$ and $-2g_0$ respectively
34	$\{0, 0, 0, e_3; 0, g_1, g_2, 0\}$	$Q=\mathbf{k}+\varepsilon(g_1\mathbf{i}+g_2\mathbf{j})$			Half-turn rotation about the Z-axis and translations along the X-axis and Y-axis with translational distance $-2g_2$ and $2g_1$ respectively
35	$\{e_0, e_1, 0, 0; 0, 0, g_2, 0\}$	$Q=e_0+e_1\mathbf{i}+\varepsilon(g_2\mathbf{j})$			Rotation by an angle $2\text{atan}(e_1, e_0)$ about the X-axis and translations along the Y-axis and Z-axis with translational distance $2e_0g_2$ and $2e_1g_2$ respectively
36	$\{e_0, e_1, 0, 0; 0, 0, 0, g_3\}$	$Q=e_0+e_1\mathbf{i}+\varepsilon(g_3\mathbf{k})$			Rotation by an angle $2\text{atan}(e_1, e_0)$ about the X-axis and translations along the Y-axis and Z-axis with translational distance $-2e_1g_3$ and $2e_0g_3$ respectively
37	$\{e_0, 0, e_2, 0;$	$Q=e_0+e_2\mathbf{j}+\varepsilon(g_1\mathbf{i})$			Rotation by an angle $2\text{atan}(e_2, e_0)$ about the Y-axis and translations along

	$0, g_1, 0, 0\}$				the X-axis and Z-axis with translational distance $2e_0g_1$ and $-2e_2g_1$ respectively.
38	$\{e_0, 0, e_2, 0;$ $0, 0, 0, g_3\}$	$Q=e_0+e_2\mathbf{j}+\varepsilon(g_3\mathbf{k})$			Rotation by an angle $2\text{atan}(e_2, e_0)$ about the Y-axis and translations along the X-axis and Z-axis with translational distance $2e_2g_3$ and $2e_0g_3$ respectively
39	$\{e_0, 0, 0, e_3;$ $0, g_1, 0, 0\}$	$Q=e_0+e_3\mathbf{k}+\varepsilon(g_1\mathbf{i})$			Rotation by an angle $2\text{atan}(e_3, e_0)$ about the Z-axis and translations along the X-axis and Y-axis with translational distance $2e_0g_1$ and $2e_3g_1$ respectively.
40	$\{e_0, 0, 0, e_3;$ $0, 0, g_2, 0\}$	$Q=e_0+e_3\mathbf{k}+\varepsilon(g_2\mathbf{j})$			Rotation by an angle $2\text{atan}(e_3, e_0)$ about the Z-axis and translations along the X-axis and Y-axis with translational distance $-2e_3g_2$ and $2e_0g_2$ respectively.
41	$\{0, e_1, e_2\ 0;$ $g_0, 0, 0, 0\}$	$Q=e_1\mathbf{i}+e_2\mathbf{j}+\varepsilon(g_0)=$ $(e_1+e_2\mathbf{k})\mathbf{i}+\varepsilon(g_0)$			Half-turn rotation about the X-axis followed by a rotation about the Z-axis by an angle $2\text{atan}(e_2, e_1)$, and translations along the X-axis and Y-axis with translational distance $-2e_1g_0$ and $-2e_2g_0$ respectively.
42	$\{0, e_1, e_2\ 0;$ $0, 0, 0, g_3\}$	$Q=e_1\mathbf{i}+e_2\mathbf{j}+\varepsilon(g_3\mathbf{k})=$ $(e_1+e_2\mathbf{k})\mathbf{i}+\varepsilon(g_3\mathbf{k})$			Half-turn rotation about the X-axis followed by a rotation about the Z-axis by an angle $2\text{atan}(e_2, e_1)$, and translations along the X-axis and Y-axis with translational distance $2e_2g_3$ and $-2e_1g_3$ respectively.
43	$\{0, e_1, 0, e_3;$ $g_0, 0, 0, 0\}$	$Q=e_1\mathbf{i}+e_3\mathbf{k}+\varepsilon(g_0)=$ $(e_1-e_3\mathbf{j})\mathbf{i}+\varepsilon(g_0)$	1	1	Half-turn rotation about the X-axis followed by a rotation by an angle $2\text{atan}(-e_3, e_1)$ about the Y-axis, and translations along the X-axis and Z-axis with translational distance $2e_1g_0$ and $-2e_3g_0$ respectively
44	$\{0, e_1, 0, e_3;$ $0, 0, g_2, 0\}$	$Q=e_1\mathbf{i}+e_3\mathbf{k}+\varepsilon(g_2\mathbf{j})=$ $(e_1-e_3\mathbf{j})\mathbf{i}+\varepsilon(g_2\mathbf{j})$			Half-turn rotation about the X-axis followed by a rotation by an angle $2\text{atan}(-e_3, e_1)$ about the Y-axis, and translations along the X-axis and Z-axis with translational distance $-2e_3g_2$ and $2e_1g_2$ respectively
45	$\{0, 0, e_2, e_3;$ $g_0, 0, 0, 0\}$	$Q=e_2\mathbf{j}+e_3\mathbf{k}+\varepsilon(g_0)=$ $(e_2+e_3\mathbf{i})\mathbf{j}+\varepsilon(g_0)$			Half-turn rotation about the Y-axis followed by a rotation by an angle $2\text{atan}(e_3, e_2)$ about the X-axis, and translations along the Y-axis and Z-axis with translational distance $-2e_2g_0$ and $-2e_3g_0$ respectively.
46	$\{0, 0, e_2, e_3;$ $0, g_1, 0, 0\}$	$Q=e_2\mathbf{j}+e_3\mathbf{k}+\varepsilon(g_1\mathbf{i})=$ $(e_2+e_3\mathbf{i})\mathbf{j}+\varepsilon(g_1\mathbf{i})$			Half-turn rotation about the Y-axis followed by a rotation by an angle $2\text{atan}(e_3, e_2)$ about the X-axis, and translations along the Y-axis and Z-axis with translational distance $2e_3g_1$ and $-2e_2g_1$ respectively.
47	$\{e_0, e_1, 0, 0;$ $g_0, g_1, 0, 0\}$	$Q=e_0+e_1\mathbf{i}+\varepsilon(g_0+g_1\mathbf{i})$			Rotation by an angle $2\text{atan}(e_1, e_0)$ about the X-axis and translation along the X-axis with translational distance $2e_0g_1$-$2e_1g_0$.
48	$\{e_0, 0, e_2, 0;$ $g_0, 0, g_2, 0\}$	$Q=e_0+e_2\mathbf{j}+\varepsilon(g_0+g_2\mathbf{j})$			Rotation by an angle $2\text{atan}(e_2, e_0)$ about the Y-axis and translation along the Y-axis with translational distance $2e_0g_2$-$2e_2g_0$.
49	$\{e_0, 0, 0, e_3;$ $g_0, 0, 0, g_3\}$	$Q=e_0+e_3\mathbf{k}+\varepsilon(g_0+g_3\mathbf{k})$			Rotation by an angle $2\text{atan}(e_3, e_0)$ about the Z-axis and translation along the Z-axis with translational distance $2e_0g_3$-$2e_3g_0$.
50	$\{0, e_1, e_2\ 0;$ $0, g_1, g_2, 0\}$	$Q=e_1\mathbf{i}+e_2\mathbf{j}+\varepsilon(g_1\mathbf{i}+g_2\mathbf{j})=$ $(e_1+e_2\mathbf{k})\mathbf{i}+\varepsilon(g_1\mathbf{i}+g_2\mathbf{j})$			Half-turn rotation about the X-axis followed by a rotation about the Z-axis by an angle $2\text{atan}(e_2, e_1)$, and translation along the Z-axis and with translational distance $2e_1g_2$-$2e_2g_1$.
51	$\{0, e_1, 0, e_3;$ $0, g_1, 0, g_3\}$	$Q=e_1\mathbf{i}+e_3\mathbf{k}+\varepsilon(g_1\mathbf{i}+g_3\mathbf{k})=$ $(e_1-e_3\mathbf{j})\mathbf{i}+\varepsilon(g_1\mathbf{i}+g_3\mathbf{k})$			Half-turn rotation about the X-axis followed by a rotation by an angle $2\text{atan}(-e_3, e_1)$ about the Y-axis, and translation along the Y-axis with translational distance $-2e_1g_3+2e_3g_1$.
52	$\{0, 0, e_2, e_3;$ $0, 0, g_2, g_3\}$	$Q=e_2\mathbf{j}+e_3\mathbf{k}+\varepsilon(g_2\mathbf{j}+g_3\mathbf{k})=$ $(e_2+e_3\mathbf{i})\mathbf{j}+\varepsilon(g_2\mathbf{j}+g_3\mathbf{k})$			Half-turn rotation about the Y-axis followed by a rotation by an angle $2\text{atan}(e_3, e_2)$ about the X-axis, and translation along the X-axis with translational distance $2e_2g_3$-$2e_3g_2$.
53	$\{e_0, e_1, e_2, 0;$ $0, 0, 0, 0\}$	$Q=e_0+e_1\mathbf{i}+e_2\mathbf{j}=(-e_2\mathbf{i}+e_1\mathbf{j}-e_0\mathbf{k})\mathbf{k}$			Half-turn rotation about the Z-axis followed by a half-turn rotation about the axis $\boldsymbol{u}=(-e_2, e_1, -e_0)^T$
54	$\{e_0, e_1, 0, e_3;$ $0, 0, 0, 0\}$	$Q=e_0+e_1\mathbf{i}+e_3\mathbf{k}=(e_3\mathbf{i}-e_0\mathbf{j}-e_1\mathbf{k})\mathbf{j}$	2	0	Half-turn rotation about the Y-axis followed by a half-turn rotation about the axis $\boldsymbol{u}=(e_3, -e_0, -e_1)^T$
55	$\{e_0, 0, e_2, e_3;$ $0, 0, 0, 0\}$	$Q=e_0+e_2\mathbf{j}+e_3\mathbf{k}=(-e_0\mathbf{i}-e_3\mathbf{j}+e_2\mathbf{k})\mathbf{i}$			Half-turn rotation about the X-axis followed by a half-turn rotation about the axis $\boldsymbol{u}=(-e_0, -e_3, e_2)^T$
56	$\{0, e_1, e_2, e_3;$ $0, 0, 0, 0\}$	$Q= e_1\mathbf{i} +e_2\mathbf{j}+e_3\mathbf{k}$			Half-turn rotation about the axis $\boldsymbol{u}=(e_1, e_2, e_3)^T$
57	$\{e_0, 0, 0, 0;$ $0, g_1, g_2, g_3\}$	$Q=1+\varepsilon(g_1\mathbf{i}+g_2\mathbf{j}+ g_3\mathbf{k})$			Translations along the X-axis, Y-axis and Z-axis with translational distance $2g_1$, $2g_2$ and $2g_3$ respectively
58	$\{0, e_1, 0, 0;$ $g_0, 0, g_2, g_3\}$	$Q=\mathbf{i}+\varepsilon(g_0+g_2\mathbf{j}+g_3\mathbf{k})$	0	3	Half-turn rotation about the X-axis and translations along the X-axis, Y-axis and Z-axis with translational distance $2g_0$, $-2g_3$ and $2g_2$ respectively
59	$\{0, 0, e_2, 0;$ $g_0, g_1, 0, g_3\}$	$Q=\mathbf{j}+\varepsilon(g_0+g_1\mathbf{i}+g_3\mathbf{k})$			Half-turn rotation about the Y-axis and translations along the X-axis, Y-axis and Z-axis with translational distance $2g_3$, $-2g_0$ and $-2g_1$ respectively
60	$\{0, 0, 0, e_3;$ $g_0, g_1, g_2, 0\}$	$Q=\mathbf{k}+\varepsilon(g_0+g_1\mathbf{i}+g_2\mathbf{j})$			Half-turn rotation about the Z-axis and translations along the X-axis, Y-axis and Z-axis with translational distance $-2g_2$, $2g_1$ and $-2g_0$ respectively
61	$\{e_0, e_1, 0, 0;$ $0, 0, g_2, g_3\}$	$Q=e_0+e_1\mathbf{i}+\varepsilon(g_2\mathbf{j}+g_3\mathbf{k})$			Rotation by an angle $2\text{atan}(e_1, e_0)$ about the X-axis and translations along the Y-axis and Z-axis with translational distance $2e_0g_2$-$2e_1g_3$ and $2e_0g_3$+$2e_1g_2$ respectively
62	$\{e_0, 0, e_2, 0;$ $0, g_1, 0, g_3\}$	$Q=e_0+e_2\mathbf{j}+\varepsilon(g_1\mathbf{i}+g_3\mathbf{k})$			Rotation by an angle $2\text{atan}(e_2, e_0)$ about the Y-axis and translations along the X-axis and Z-axis with translational distance $2e_0g_1$+$2e_2g_3$ and $2e_0g_3$-$2e_2g_1$ respectively
63	$\{e_0, 0, 0, e_3;$ $0, g_1, g_2, 0\}$	$Q=e_0+e_3\mathbf{k}+\varepsilon(g_1\mathbf{i}+g_2\mathbf{j})$			Rotation by an angle $2\text{atan}(e_3, e_0)$ about the Z-axis and translations along the X-axis and Y-axis with translational distance $2e_0g_1$-$2e_3g_2$ and $2e_0g_2$+$2e_3g_1$ respectively.
64	$\{0, e_1, e_2\ 0;$ $g_0, 0, 0, g_3\}$	$Q=e_1\mathbf{i}+e_2\mathbf{j}+\varepsilon(g_0+g_3\mathbf{k})=$ $(e_1+e_2\mathbf{k})\mathbf{i}+\varepsilon(g_0+g_3\mathbf{k})$			Half-turn rotation about the X-axis followed by a rotation about Z-axis by an angle $2\text{atan}(e_2, e_1)$, and translations along the X-axis and Y-axis with translational distance $-2e_1g_0$+$2e_2g_3$ and $-2e_1g_3$-$2e_2g_0$ respectively.
65	$\{0, e_1, 0, e_3;$ $g_0, 0, g_2, 0\}$	$Q=e_1\mathbf{i}+e_3\mathbf{k}+\varepsilon(g_0+g_2\mathbf{j})=$ $(e_1-e_3\mathbf{j})\mathbf{i}+\varepsilon(g_0+g_2\mathbf{j})$			Half-turn rotation about the X-axis followed by a rotation by an angle $2\text{atan}(-e_3, e_1)$ about the Y-axis, and translations along the X-axis and Z-axis with translational distance $-2e_1g_0$-$2e_3g_2$ and $2e_1g_2$-$2e_3g_0$ respectively

66	{0, 0, e_2, e_3; g_0, g_1, 0, 0}	$Q=e_2\mathbf{j}+e_3\mathbf{k}+\varepsilon(g_0+g_1\mathbf{i})=(e_2+e_3\mathbf{i})\mathbf{j}+\varepsilon(g_0+g_1\mathbf{i})$	1	2	Half-turn rotation about the Y-axis followed by a rotation by an angle 2atan(e_3, e_2) about the X-axis, and translations along the Y-axis and Z-axis with translational distance $-2e_2g_0+2e_3g_1$ and $-2e_2g_1-2e_3g_0$ respectively.
67	{e_0, e_1, 0, 0; g_0, g_1, g_2, 0}	$Q=e_0+e_1\mathbf{i}+\varepsilon(g_0+g_1\mathbf{i}+g_2\mathbf{j})$			Rotation by an angle 2atan(e_1, e_0) about the X-axis and translations along the X-axis, Y-axis and Z-axis with translational distance $2e_0g_1-2e_1g_0$, $2e_0g_2$ and $2e_1g_2$ respectively.
68	{e_0, e_1, 0, 0; g_0, g_1, 0, g_3}	$Q=e_0+e_1\mathbf{i}+\varepsilon(g_0+g_1\mathbf{i}+g_3\mathbf{k})$			Rotation by an angle 2atan(e_1, e_0) about the X-axis and translations along the X-axis, Y-axis and Z-axis with translational distance $2e_0g_1-2e_1g_0$, $-2e_1g_3$ and $2e_0g_3$ respectively.
69	{e_0, 0, e_2, 0; g_0, g_1, g_2, 0}	$Q=e_0+e_2\mathbf{j}+\varepsilon(g_0+g_1\mathbf{i}+g_2\mathbf{j})$			Rotation by an angle 2atan(e_2, e_0) about the Y-axis and translations along the X-axis, Y-axis and Z-axis with translational distance $2e_0g_1$, $2e_0g_2-2e_2g_0$ and $-2e_2g_1$ respectively.
70	{e_0, 0, e_2, 0; g_0, 0, g_2, g_3}	$Q=e_0+e_2\mathbf{j}+\varepsilon(g_0+g_2\mathbf{j}+g_3\mathbf{k})$			Rotation by an angle 2atan(e_2, e_0) about the Y-axis and translations along the X-axis, Y-axis and Z-axis with translational distance $2e_2g_3$, $2e_0g_2-2e_2g_0$ and $2e_0g_3$ respectively.
71	{e_0, 0, 0, e_3; g_0, g_1, 0, g_3}	$Q=e_0+e_3\mathbf{k}+\varepsilon(g_0+g_1\mathbf{i}+g_3\mathbf{k})$			Rotation by an angle 2atan(e_3, e_0) about the Z-axis and translations along the X-axis, Y-axis and Z-axis with translational distance $2e_0g_1$, $2e_3g_1$ and $2e_0g_3-2e_3g_0$ respectively.
72	{e_0, 0, 0, e_3; g_0, 0, g_2, g_3}	$Q=e_0+e_3\mathbf{k}+\varepsilon(g_0+g_2\mathbf{j}+g_3\mathbf{k})$			Rotation by an angle 2atan(e_3, e_0) about the Z-axis and translations along the X-axis, Y-axis and Z-axis with translational distance $-2e_3g_2$, $2e_0g_2$ and $2e_0g_3-2e_3g_0$ respectively.
73	{0, e_1, e_2 0; g_0, g_1, g_2, 0}	$Q=e_1\mathbf{i}+e_2\mathbf{j}+\varepsilon(g_0+g_1\mathbf{i}+g_2\mathbf{j})=(e_1+e_2\mathbf{k})\mathbf{i}+\varepsilon(g_0+g_1\mathbf{i}+g_2\mathbf{j})$			Half-turn rotation about the X-axis followed by a rotation about the Z-axis by an angle 2atan(e_2, e_1), and translations along the X-axis, Y-axis and Z-axis with translational distance $-2e_1g_0$, $-2e_2g_0$ and $2e_1g_2-2e_2g_1$ respectively.
74	{0, e_1, e_2 0; 0, g_1, g_2, g_3}	$Q=e_1\mathbf{i}+e_2\mathbf{j}+\varepsilon(g_1\mathbf{i}+g_2\mathbf{j}+g_3\mathbf{k})=(e_1+e_2\mathbf{k})\mathbf{i}+\varepsilon(g_1\mathbf{i}+g_2\mathbf{j}+g_3\mathbf{k})$			Half-turn rotation about the X-axis followed by a rotation about the Z-axis by 2atan(e_2, e_1), and translations along the X-axis, Y-axis and Z-axis with translational distance $2e_2g_3$, $-2e_1g_3$ and $2e_1g_2-2e_2g_1$ respectively.
75	{0, e_1, 0, e_3; g_0, g_1, 0, g_3}	$Q=e_1\mathbf{i}+e_3\mathbf{k}+\varepsilon(g_0+g_1\mathbf{i}+g_3\mathbf{k})=(e_1-e_3\mathbf{j})\mathbf{i}+\varepsilon(g_0+g_1\mathbf{i}+g_3\mathbf{k})$			Half-turn rotation about the X-axis followed by a rotation by an angle 2atan($-e_3$, e_1) about the Y-axis, and translations along the X-axis, Y-axis and Z-axis with translational distance $-2e_1g_0$, $-2e_1g_3-2e_3g_1$ and $-2e_3g_0$ respectively.
76	{0, e_1, 0, e_3; 0, g_1, g_2, g_3}	$Q=e_1\mathbf{i}+e_3\mathbf{k}+\varepsilon(g_1\mathbf{i}+g_2\mathbf{j}+g_3\mathbf{k})=(e_1-e_3\mathbf{j})\mathbf{i}+\varepsilon(g_1\mathbf{i}+g_2\mathbf{j}+g_3\mathbf{k})$			Half-turn rotation about the X-axis followed by a rotation by an angle 2atan($-e_3$, e_1) about the Y-axis, and translations along the X-axis, Y-axis and Z-axis with translational distance $-2e_3g_2$, $-2e_1g_3-2e_3g_1$ and $2e_1g_2$ respectively.
77	{0, 0, e_2, e_3; g_0, 0, g_2, g_3}	$Q=e_2\mathbf{j}+e_3\mathbf{k}+\varepsilon(g_0+g_2\mathbf{j}+g_3\mathbf{k})=(e_2+e_3\mathbf{i})\mathbf{j}+\varepsilon(g_0+g_2\mathbf{j}+g_3\mathbf{k})$			Half-turn rotation about the Y-axis followed by a rotation by an angle 2atan(e_3, e_2) about the X-axis, and translations along the X-axis, Y-axis and Z-axis with translational distance $2e_2g_3-2e_3g_2$, $-2e_2g_0$ and $-2e_3g_0$ respectively.
78	{0, 0, e_2, e_3; 0, g_1, g_2, g_3}	$Q=e_2\mathbf{j}+e_3\mathbf{k}+\varepsilon(g_1\mathbf{i}+g_2\mathbf{j}+g_3\mathbf{k})=(e_2+e_3\mathbf{i})\mathbf{j}+\varepsilon(g_1\mathbf{i}+g_2\mathbf{j}+g_3\mathbf{k})$			Half-turn rotation about the Y-axis followed by a rotation by an angle 2atan(e_3, e_2) about the X-axis, and translations along the X-axis, Y-axis and Z-axis with translational distance $2e_2g_3-2e_3g_2$, $2e_3g_1$ and $2e_3g_1$ respectively.
79	{e_0, e_1, e_2, 0; 0, 0, 0, g_3}	$Q=e_0+e_1\mathbf{i}+e_2\mathbf{j}+\varepsilon(g_3\mathbf{k})=(-e_2\mathbf{i}+e_1\mathbf{j}-e_0\mathbf{k})\mathbf{k}+\varepsilon(g_3\mathbf{k})$			Half-turn rotation about the Z-axis followed by a half-turn rotation about the axis $\boldsymbol{u}=(-e_2, e_1, -e_0)^T$, and translations along the X-axis, Y-axis and Z-axis with translational distance $2e_2g_3$, $-2e_1g_3$ and $2e_0g_3$ respectively.
80	{e_0, e_1, 0, e_3; 0, 0, g_2, 0}	$Q=e_0+e_1\mathbf{i}+e_3\mathbf{k}+\varepsilon(g_2\mathbf{j})=(e_3\mathbf{i}-e_0\mathbf{j}-e_1\mathbf{k})\mathbf{j}+\varepsilon(g_2\mathbf{j})$			Half-turn rotation about the Y-axis followed by a half-turn rotation about the axis $\boldsymbol{u}=(e_3, -e_0, -e_1)^T$, and translations along the X-axis, Y-axis and Z-axis with translational distance $-2e_3g_2$, $2e_0g_2$ and $2e_1g_2$ respectively.
81	{e_0, 0, e_2, e_3; 0, g_1, 0, 0}	$Q=e_0+e_2\mathbf{j}+e_3\mathbf{k}+\varepsilon(g_1\mathbf{i})=(-e_0\mathbf{i}-e_3\mathbf{j}+e_2\mathbf{k})\mathbf{i}+\varepsilon(g_1\mathbf{i})$			Half-turn rotation about the X-axis followed by a half-turn rotation about the axis $\boldsymbol{u}=(-e_0, -e_3, e_2)^T$, and translations along the X-axis, Y-axis and Z-axis with translational distance $2e_0g_1$, $2e_3g_1$ and $-2e_2g_1$ respectively.
82	{0, e_1, e_2, e_3; g_0, 0, 0, 0}	$Q=e_1\mathbf{i}+e_2\mathbf{j}+e_3\mathbf{k}+\varepsilon(g_0)$			Half-turn rotation about the axis $\boldsymbol{u}=(e_1, e_2, e_3)^T$ and translations along the X-axis, Y-axis and Z-axis with translational distance $-2e_1g_0$, $-2e_2g_0$ and $-2e_3g_0$ respectively.
83	{e_0, e_1, e_2, 0; g_0, g_1, 0, 0}	$Q=e_0+e_1\mathbf{i}+e_2\mathbf{j}+\varepsilon(g_0+g_1\mathbf{i})=(-e_2\mathbf{i}+e_1\mathbf{j}-e_0\mathbf{k})\mathbf{k}+\varepsilon(g_0+g_1\mathbf{i})$			Half-turn rotation about the Z-axis followed by a half-turn rotation about the axis $\boldsymbol{u}=(-e_2, e_1, -e_0)^T$, and translations along the X-axis, Y-axis and Z-axis with translational distance $2e_0g_1-2e_1g_0$, $-2e_2g_0$ and $-2e_2g_1$ respectively.
84	{e_0, e_1, e_2, 0; g_0, 0, g_2, 0}	$Q=e_0+e_1\mathbf{i}+e_2\mathbf{j}+\varepsilon(g_0+g_2\mathbf{j})=(-e_2\mathbf{i}+e_1\mathbf{j}-e_0\mathbf{k})\mathbf{k}+\varepsilon(g_0+g_2\mathbf{j})$			Half-turn rotation about the Z-axis followed by a half-turn rotation about the axis $\boldsymbol{u}=(-e_2, e_1, -e_0)^T$, and translations along the X-axis, Y-axis and Z-axis with translational distance $-2e_1g_0$, $2e_0g_2-2e_2g_0$ and $2e_1g_2$ respectively.
85	{e_0, e_1, e_2, 0; 0, g_1, g_2, 0}	$Q=e_0+e_1\mathbf{i}+e_2\mathbf{j}+\varepsilon(g_1\mathbf{i}+g_2\mathbf{j})=(-e_2\mathbf{i}+e_1\mathbf{j}-e_0\mathbf{k})\mathbf{k}+\varepsilon(g_0+g_2\mathbf{j})$			Half-turn rotation about the Z-axis followed by a half-turn rotation about the axis $\boldsymbol{u}=(-e_2, e_1, -e_0)^T$, and translations along the X-axis, Y-axis and Z-axis with translational distance $2e_0g_1$, $2e_0g_2$ and $2e_1g_2-2e_2g_1$ respectively.
86	{e_0, e_1, 0, e_3; g_0, g_1, 0, 0}	$Q=e_0+e_1\mathbf{i}+e_3\mathbf{k}+\varepsilon(g_0+g_1\mathbf{i})=(e_3\mathbf{i}-e_0\mathbf{j}-e_1\mathbf{k})\mathbf{j}+\varepsilon(g_0+g_1\mathbf{i})$			Half-turn rotation about the Y-axis followed by a half-turn rotation about the axis $\boldsymbol{u}=(e_3, -e_0, -e_1)^T$, and translations along the X-axis, Y-axis and Z-axis with translational distance $2e_0g_1-2e_1g_0$, $2e_3g_1$ and $-2e_3g_0$ respectively.
87	{e_0, e_1, 0, e_3; g_0, 0, 0, g_3}	$Q=e_0+e_1\mathbf{i}+e_3\mathbf{k}+\varepsilon(g_0+g_3\mathbf{k})=(e_3\mathbf{i}-e_0\mathbf{j}-e_1\mathbf{k})\mathbf{j}+\varepsilon(g_0+g_3\mathbf{k})$	2	1	Half-turn rotation about the Y-axis followed by a half-turn rotation about the axis $\boldsymbol{u}=(e_3, -e_0, -e_1)^T$, and translations along the X-axis, Y-axis and Z-axis with translational distance $-2e_1g_0$, $-2e_1g_3$ and $2e_0g_3-2e_3g_0$ respectively.

88	$\{e_0, e_1, 0, e_3; 0, g_1, 0, g_3\}$	$Q=e_0+e_1\mathbf{i}+e_3\mathbf{k}+\varepsilon(g_1\mathbf{i}+g_3\mathbf{k})=(e_3\mathbf{i}-e_0\mathbf{j}-e_1\mathbf{k})\mathbf{j}+\varepsilon(g_1\mathbf{i}+g_3\mathbf{k})$			Half-turn rotation about the Y-axis followed by a half-turn rotation about the axis $\boldsymbol{u}=(e_3, -e_0, -e_1)^T$, and translations along the X-axis, Y-axis and Z-axis with translational distance $2e_0g_1$, $-2e_1g_3+2e_3g_1$ and $2e_0g_3$ respectively.
89	$\{e_0, 0, e_2, e_3; g_0, 0, g_2, 0\}$	$Q=e_0+e_2\mathbf{j}+e_3\mathbf{k}+\varepsilon(g_0+g_2\mathbf{j})=(-e_0\mathbf{i}-e_3\mathbf{j}+e_2\mathbf{k})\mathbf{i}+\varepsilon(g_0+g_2\mathbf{j})$			Half-turn rotation about the X-axis followed by a half-turn rotation about the axis $\boldsymbol{u}=(-e_0, -e_3, e_2)^T$, and translations along the X-axis, Y-axis and Z-axis with translational distance $-2e_3g_2$, $2e_0g_2-2e_2g_0$ and $-2e_3g_0$ respectively.
90	$\{e_0, 0, e_2, e_3; g_0, 0, 0, g_3\}$	$Q=e_0+e_2\mathbf{j}+e_3\mathbf{k}+\varepsilon(g_0+g_3\mathbf{k})=(-e_0\mathbf{i}-e_3\mathbf{j}+e_2\mathbf{k})\mathbf{i}+\varepsilon(g_0+g_3\mathbf{k})$			Half-turn rotation about the X-axis followed by a half-turn rotation about the axis $\boldsymbol{u}=(-e_0, -e_3, e_2)^T$, and translations along the X-axis, Y-axis and Z-axis with translational distance $2e_2g_3$, $-2e_2g_0$ and $2e_0g_3-2e_3g_0$ respectively.
91	$\{e_0, 0, e_2, e_3; 0, 0, g_2, g_3\}$	$Q=e_0+e_2\mathbf{j}+e_3\mathbf{k}+\varepsilon(g_2\mathbf{j}+g_3\mathbf{k})=(-e_0\mathbf{i}-e_3\mathbf{j}+e_2\mathbf{k})\mathbf{i}+\varepsilon(g_2\mathbf{j}+g_3\mathbf{k})$			Half-turn rotation about the X-axis followed by a half-turn rotation about the axis $\boldsymbol{u}=(-e_0, -e_3, e_2)^T$, and translations along the X-axis, Y-axis and Z-axis with translational distance $2e_2g_3-2e_3g_2$, $2e_0g_2$ and $2e_0g_3$ respectively.
92	$\{0, e_1, e_2, e_3; 0, g_1, g_2, 0\}$	$Q=e_1\mathbf{i}+e_2\mathbf{j}+e_3\mathbf{k}+\varepsilon(g_1\mathbf{i}+g_2\mathbf{j})$			Half-turn rotation about the axis $\boldsymbol{u}=(e_1, e_2, e_3)^T$ and translations along the X-axis, Y-axis and Z-axis with translational distance $-2e_3g_2$, $2e_3g_1$ and $2e_1g_2-2e_2g_1$ respectively.
93	$\{0, e_1, e_2, e_3; 0, g_1, 0, g_3\}$	$Q=e_1\mathbf{i}+e_2\mathbf{j}+e_3\mathbf{k}+\varepsilon(g_1\mathbf{i}+g_3\mathbf{k})$			Half-turn rotation about the axis $\boldsymbol{u}=(e_1, e_2, e_3)^T$ and translations along the X-axis, Y-axis and Z-axis with translational distance $2e_2g_3$, $-2e_1g_3+2e_3g_1$ and $-2e_2g_1$ respectively.
94	$\{0, e_1, e_2, e_3; 0, 0, g_2, g_3\}$	$Q=e_1\mathbf{i}+e_2\mathbf{j}+e_3\mathbf{k}+\varepsilon(g_2\mathbf{j}+g_3\mathbf{k})$			Half-turn rotation about the axis $\boldsymbol{u}=(e_1, e_2, e_3)^T$ and translations along the X-axis, Y-axis and Z-axis with translational distance $2e_2g_3-2e_3g_2$, $-2e_1g_3$ and $2e_1g_2$ respectively.
95	$\{e_0, e_1, e_2, e_3; 0, 0, 0, 0\}$	$Q=e_0+e_1\mathbf{i}+e_2\mathbf{j}+e_3\mathbf{k}$	3	0	Spherical motion
96	$\{e_0, e_1, 0, 0; g_0, g_1, g_2, g_3\}$	$Q=e_0+e_1\mathbf{i}+\varepsilon(g_0+g_1\mathbf{i}+g_2\mathbf{j}+g_3\mathbf{k})$			Rotation by an angle $2\text{atan}(e_1, e_0)$ about the X-axis and translations along the X-axis, Y-axis and Z-axis with translational distance $2e_0g_1-2e_1g_0$, $2e_0g_2-2e_1g_3$ and $2e_0g_3+2e_1g_2$ respectively.

97	$\{e_0, 0, e_2, 0; g_0, g_1, g_2, g_3\}$	$Q=e_0+e_2\mathbf{j}+\varepsilon(g_0+g_1\mathbf{i}+g_2\mathbf{j}+g_3\mathbf{k})$			Rotation by an angle $2\text{atan}(e_2, e_0)$ about the Y-axis and translations along the X-axis, Y-axis and Z-axis with translational distance $2e_0g_1+2e_2g_3$, $2e_0g_2-2e_2g_0$ and $2e_0g_3-2e_2g_1$ respectively.
98	$\{e_0, 0, 0, e_3; g_0, g_1, g_2, g_3\}$	$Q=e_0+e_3\mathbf{k}+\varepsilon(g_0+g_1\mathbf{i}+g_2\mathbf{j}+g_3\mathbf{k})$			Rotation by an angle $2\text{atan}(e_3, e_0)$ about the Z-axis and translations along the X-axis, Y-axis and Z-axis with translational distance $2e_0g_1-2e_3g_2$, $2e_0g_2+2e_3g_1$ and $2e_0g_3-2e_3g_0$ respectively.
99	$\{0, e_1, e_2\ 0; g_0, g_1, g_2, g_3\}$	$Q=e_1\mathbf{i}+e_2\mathbf{j}+\varepsilon(g_0+g_1\mathbf{i}+g_2\mathbf{j}+g_3\mathbf{k})=(e_1+e_2\mathbf{k})\mathbf{i}+\varepsilon(g_0+g_1\mathbf{i}+g_2\mathbf{j}+g_3\mathbf{k})$	1	3	Half-turn rotation about the X-axis followed by a rotation about the Z-axis by an angle $2\text{atan}(e_2, e_1)$, and translations along the X-axis, Y-axis and Z-axis with translational distance $-2e_1g_0+2e_2g_3$, $-2e_1g_3-2e_2g_0$ and $2e_1g_2-2e_2g_1$ respectively.
100	$\{0, e_1, 0, e_3; g_0, g_1, g_2, g_3\}$	$Q=e_1\mathbf{i}+e_3\mathbf{k}+\varepsilon(g_0+g_1\mathbf{i}+g_2\mathbf{j}+g_3\mathbf{k})=(e_1-e_3\mathbf{j})\mathbf{i}+\varepsilon(g_0+g_1\mathbf{i}+g_2\mathbf{j}+g_3\mathbf{k})$			Half-turn rotation about the X-axis followed by a rotation by an angle $2\text{atan}(-e_3, e_1)$ about the Y-axis, and translations along the X-axis, Y-axis and Z-axis with translational distance $-2e_1g_0-2e_3g_2$, $-2e_1g_3-2e_3g_1$ and $2e_1g_2-2e_3g_0$ respectively.
101	$\{0, 0, e_2, e_3; g_0, g_1, g_2, g_3\}$	$Q=e_2\mathbf{j}+e_3\mathbf{k}+\varepsilon(g_0+g_1\mathbf{i}+g_2\mathbf{j}+g_3\mathbf{k})=(e_2+e_3\mathbf{i})\mathbf{j}+\varepsilon(g_0+g_1\mathbf{i}+g_2\mathbf{j}+g_3\mathbf{k})$			Half-turn rotation about the Y-axis followed by a rotation by an angle $2\text{atan}(e_3, e_2)$ about the X-axis, and translations along the X-axis, Y-axis and Z-axis with translational distance $2e_2g_3-2e_3g_2$, $-2e_2g_0+2e_3g_1$ and $-2e_2g_1-2e_3g_0$ respectively.
102	$\{e_0, e_1, e_2, 0; g_0, g_1, g_2, 0\}$	$Q=e_0+e_1\mathbf{i}+e_2\mathbf{j}+\varepsilon(g_0+g_1\mathbf{i}+g_2\mathbf{j})=(-e_2\mathbf{i}+e_1\mathbf{j}-e_0\mathbf{k})\mathbf{k}+\varepsilon(g_0+g_1\mathbf{i}+g_2\mathbf{j})$			Half-turn rotation about the Z-axis followed by a half-turn rotation about the axis $\boldsymbol{u}=(-e_2, e_1, -e_0)^T$, and translations along the X-axis, Y-axis and Z-axis with translational distance $2e_0g_1-2e_1g_0$, $2e_0g_2-2e_2g_0$ and $2e_1g_2-2e_2g_1$ respectively.
103	$\{e_0, e_1, 0, e_3; g_0, g_1, 0, g_3\}$	$Q=e_0+e_1\mathbf{i}+e_3\mathbf{k}+\varepsilon(g_0+g_1\mathbf{i}+g_3\mathbf{k})=(e_3\mathbf{i}-e_0\mathbf{j}-e_1\mathbf{k})\mathbf{j}+\varepsilon(g_0+g_1\mathbf{i}+g_3\mathbf{k})$			Half-turn rotation about the Y-axis followed by a half-turn rotation about the axis $\boldsymbol{u}=(e_3, -e_0, -e_1)^T$, and translations along the X-axis, Y-axis and Z-axis with translational distance $2e_0g_1-2e_1g_0$, $-2e_1g_3+2e_3g_1$ and $2e_0g_3-2e_3g_0$ respectively.
104	$\{e_0, 0, e_2, e_3; g_0, 0, g_2, g_3\}$	$Q=e_0+e_2\mathbf{j}+e_3\mathbf{k}+\varepsilon(g_0+g_2\mathbf{j}+g_3\mathbf{k})=(-e_0\mathbf{i}-e_3\mathbf{j}+e_2\mathbf{k})\mathbf{i}+\varepsilon(g_0+g_2\mathbf{j}+g_3\mathbf{k})$			Half-turn rotation about the X-axis followed by a half-turn rotation about the axis $\boldsymbol{u}=(-e_0, -e_3, e_2)^T$, and translations along the X-axis, Y-axis and Z-axis with translational distance $2e_2g_3-2e_3g_2$, $2e_0g_2-2e_2g_0$ and $2e_0g_3-2e_3g_0$ respectively.
105	$\{0, e_1, e_2, e_3; 0, g_1, g_2, g_3\}$	$Q=e_1\mathbf{i}+e_2\mathbf{j}+e_3\mathbf{k}+\varepsilon(g_1\mathbf{i}+g_2\mathbf{j}+g_3\mathbf{k})$			Half-turn rotation about the axis $\boldsymbol{u}=(e_1, e_2, e_3)^T$ and translations along the X-axis, Y-axis and Z-axis with translational distance $2e_2g_3-2e_3g_2$, $-2e_1g_3+2e_3g_1$ and $2e_1g_2-2e_2g_1$ respectively.
106	$\{e_0, e_1, e_2, 0; g_0, g_1, 0, g_3\}$	$Q=e_0+e_1\mathbf{i}+e_2\mathbf{j}+\varepsilon(g_0+g_1\mathbf{i}+g_3\mathbf{k})=(-e_2\mathbf{i}+e_1\mathbf{j}-e_0\mathbf{k})\mathbf{k}+\varepsilon(g_0+g_1\mathbf{i}+g_3\mathbf{k})$			Half-turn rotation about the Z-axis followed by a half-turn rotation about the axis $\boldsymbol{u}=(-e_2, e_1, -e_0)^T$, and translations along the X-axis, Y-axis and Z-axis with translational distance $2e_0g_1-2e_1g_0+2e_2g_3$, $-2e_1g_3-2e_2g_0$ and $2e_0g_3-2e_2g_1$ respectively.
107	$\{e_0, e_1, e_2, 0; g_0, 0, g_2, g_3\}$	$Q=e_0+e_1\mathbf{i}+e_2\mathbf{j}+\varepsilon(g_0+g_2\mathbf{j}+g_3\mathbf{k})=(-e_2\mathbf{i}+e_1\mathbf{j}-e_0\mathbf{k})\mathbf{k}+\varepsilon(g_0+g_2\mathbf{j}+g_3\mathbf{k})$			Half-turn rotation about the Z-axis followed by a half-turn rotation about the axis $\boldsymbol{u}=(-e_2, e_1, -e_0)^T$, and translations along the X-axis, Y-axis and Z-axis with translational distance $-2e_1g_0+2e_2g_3$, $2e_0g_2-2e_1g_3-2e_2g_0$ and $2e_1g_2+2e_0g_3$ respectively.
108	$\{e_0, e_1, e_2, 0; 0, g_1, g_2, g_3\}$	$Q=e_0+e_1\mathbf{i}+e_2\mathbf{j}+\varepsilon(g_1\mathbf{i}+g_2\mathbf{j}+g_3\mathbf{k})=(-e_2\mathbf{i}+e_1\mathbf{j}-e_0\mathbf{k})\mathbf{k}+\varepsilon(g_0+g_1\mathbf{i}+g_3\mathbf{k})$			Half-turn rotation about the Z-axis followed by a half-turn rotation about the axis $\boldsymbol{u}=(-e_2, e_1, -e_0)^T$, and translations along the X-axis, Y-axis and Z-axis with translational distance $2e_0g_1+2e_2g_3$, $2e_0g_2-2e_1g_3$ and $2e_0g_3+2e_1g_2-2e_2g_1$ respectively.
109	$\{e_0, e_1, 0, e_3; g_0, g_1, g_2, 0\}$	$Q=e_0+e_1\mathbf{i}+e_3\mathbf{k}+\varepsilon(g_0+g_1\mathbf{i}+g_2\mathbf{j})=(e_3\mathbf{i}-e_0\mathbf{j}-e_1\mathbf{k})\mathbf{j}+\varepsilon(g_0+g_1\mathbf{i}+g_2\mathbf{j})$			Half-turn rotation about the Y-axis followed by a half-turn rotation about the axis $\boldsymbol{u}=(e_3, -e_0, -e_1)^T$, and translations along the X-axis, Y-axis and Z-axis with translational distance $2e_0g_1-2e_1g_0-2e_3g_2$, $2e_0g_2+2e_3g_1$ and $2e_1g_2-2e_3g_0$ respectively.
110	$\{e_0, e_1, 0, e_3; g_0, 0, g_2, g_3\}$	$Q=e_0+e_1\mathbf{i}+e_3\mathbf{k}+\varepsilon(g_0+g_2\mathbf{j}+g_3\mathbf{k})=(e_3\mathbf{i}-e_0\mathbf{j}-e_1\mathbf{k})\mathbf{j}+\varepsilon(g_0+g_2\mathbf{j}+g_3\mathbf{k})$	2	2	Half-turn rotation about the Y-axis followed by a half-turn rotation about the axis $\boldsymbol{u}=(e_3, -e_0, -e_1)^T$, and translations along the X-axis, Y-axis and Z-axis with translational distance $-2e_1g_0-2e_3g_2$, $2e_0g_2-2e_1g_3$ and $2e_0g_3+2e_1g_2-2e_3g_0$ respectively.
111	$\{e_0, e_1, 0, e_3; 0, g_1, g_2, g_3\}$	$Q=e_0+e_1\mathbf{i}+e_3\mathbf{k}+\varepsilon(g_1\mathbf{i}+g_2\mathbf{j}+g_3\mathbf{k})=(e_3\mathbf{i}-e_0\mathbf{j}-e_1\mathbf{k})\mathbf{j}+\varepsilon(g_1\mathbf{i}+g_2\mathbf{j}+g_3\mathbf{k})$			Half-turn rotation about the Y-axis followed by a half-turn rotation about the axis $\boldsymbol{u}=(e_3, -e_0, -e_1)^T$, and translations along the X-axis, Y-axis and Z-axis with translational distance $2e_0g_1-2e_3g_2$, $2e_0g_2-2e_1g_3+2e_3g_1$ and $2e_0g_3+2e_1g_2$ respectively.
112	$\{e_0, 0, e_2, e_3; g_0, g_1, g_2, 0\}$	$Q=e_0+e_2\mathbf{j}+e_3\mathbf{k}+\varepsilon(g_0+g_1\mathbf{i}+g_2\mathbf{j})=(-e_0\mathbf{i}-e_3\mathbf{j}+e_2\mathbf{k})\mathbf{i}+\varepsilon(g_0+g_1\mathbf{i}+g_2\mathbf{j})$			Half-turn rotation about the X-axis followed by a half-turn rotation about the axis $\boldsymbol{u}=(-e_0, -e_3, e_2)^T$, and translations along the X-axis, Y-axis and Z-axis with translational distance $2e_0g_1-2e_3g_2$, $2e_0g_2-2e_2g_0+2e_3g_1$ and $-2e_2g_1-2e_3g_0$ respectively.
113	$\{e_0, 0, e_2, e_3; g_0, g_1, 0, g_3\}$	$Q=e_0+e_2\mathbf{j}+e_3\mathbf{k}+\varepsilon(g_0+g_1\mathbf{i}+g_3\mathbf{k})=(-e_0\mathbf{i}-e_3\mathbf{j}+e_2\mathbf{k})\mathbf{i}+\varepsilon(g_0+g_1\mathbf{i}+g_3\mathbf{k})$			Half-turn rotation about the X-axis followed by a half-turn rotation about the axis $\boldsymbol{u}=(-e_0, -e_3, e_2)^T$, and translations along the X-axis, Y-axis and Z-axis with translational distance $2e_0g_1+2e_2g_3$, $-2e_2g_0+2e_3g_1$ and $2e_0g_3-2e_2g_1-2e_3g_0$ respectively.
114	$\{e_0, 0, e_2, e_3; 0, g_1, g_2, g_3\}$	$Q=e_0+e_2\mathbf{j}+e_3\mathbf{k}+\varepsilon(g_1\mathbf{i}+g_2\mathbf{j}+g_3\mathbf{k})=(-e_0\mathbf{i}-e_3\mathbf{j}+e_2\mathbf{k})\mathbf{i}+\varepsilon(g_1\mathbf{i}+g_2\mathbf{j}+g_3\mathbf{k})$			Half-turn rotation about the X-axis followed by a half-turn rotation about the axis $\boldsymbol{u}=(-e_0, -e_3, e_2)^T$, and translations along the X-axis, Y-axis and Z-axis with translational distance $2e_0g_1+2e_2g_3-2e_3g_2$, $2e_0g_2+2e_3g_1$ and $2e_0g_3-2e_2g_1$ respectively.
115	$\{0, e_1, e_2, e_3; g_0, g_1, g_2, 0\}$	$Q=e_1\mathbf{i}+e_2\mathbf{j}+e_3\mathbf{k}+\varepsilon(g_0+g_1\mathbf{i}+g_2\mathbf{j})$			Half-turn rotation about the axis $\boldsymbol{u}=(e_1, e_2, e_3)^T$ and translations along the X-axis, Y-axis and Z-axis with translational distance $-2e_1g_0-2e_3g_2$, $-2e_2g_0+2e_3g_1$ and $2e_1g_2-2e_2g_1-2e_3g_0$ respectively.
116	$\{0, e_1, e_2, e_3; g_0, g_1, 0, g_3\}$	$Q=e_1\mathbf{i}+e_2\mathbf{j}+e_3\mathbf{k}+\varepsilon(g_0+g_1\mathbf{i}+g_3\mathbf{k})$			Half-turn rotation about the axis $\boldsymbol{u}=(e_1, e_2, e_3)^T$ and translations along the X-axis, Y-axis and Z-axis with translational distance $-2e_1g_0+2e_2g_3$, $-2e_1g_3-2e_2g_0+2e_3g_1$ and $-2e_2g_1-2e_3g_0$ respectively.
117	$\{0, e_1, e_2, e_3;$	$Q=e_1\mathbf{i}+e_2\mathbf{j}+e_3\mathbf{k}+\varepsilon(g_0+g_2\mathbf{j}+g_3\mathbf{k})$			Half-turn rotation about the axis $\boldsymbol{u}=(e_1, e_2, e_3)^T$ and translations along the

Mechanism and Machine Theory, 2019, Vol 142, 103577
https://doi.org/10.1016/j.mechmachtheory.2019.103577

$g_0, 0, g_2, g_3\}$	X-axis, Y-axis and Z-axis with translational distance $-2e_1g_0+2e_2g_3-2e_3g_2$, $-2e_1g_3-2e_2g_0$ and $2e_1g_2-2e_3g_0$ respectively.

118	$\{e_0, e_1, e_2, e_3; g_0, g_1, 0, 0\}$	$Q=e_0+e_1\mathbf{i}+e_2\mathbf{j}+e_3\mathbf{k}+\varepsilon(g_0+g_1\mathbf{i})$	3	1	Spherical motion and translations along the *X*-axis, *Y*-axis and *Z*-axis with translational distance $2e_0g_1-2e_1g_0$, $-2e_2g_0+2e_3g_1$ and $-2e_2g_1-2e_3g_0$ respectively.
119	$\{e_0, e_1, e_2, e_3; g_0, 0, g_2, 0\}$	$Q=e_0+e_1\mathbf{i}+e_2\mathbf{j}+e_3\mathbf{k}+\varepsilon(g_0+g_2\mathbf{j})$			Spherical motion and translations along the *X*-axis, *Y*-axis and *Z*-axis with translational distance $-2e_1g_0-2e_3g_2$, $2e_0g_2-2e_2g_0$ and $2e_1g_2-2e_3g_0$ respectively.
120	$\{e_0, e_1, e_2, e_3; g_0, 0, 0, g_3\}$	$Q=e_0+e_1\mathbf{i}+e_2\mathbf{j}+e_3\mathbf{k}+\varepsilon(g_0+g_3\mathbf{k})$			Spherical motion and translations along the *X*-axis, *Y*-axis and *Z*-axis with translational distance $-2e_1g_0+2e_2g_3$, $-2e_1g_3-2e_2g_0$ and $2e_0g_3-2e_3g_0$ respectively.
121	$\{e_0, e_1, e_2, e_3; 0, g_1, g_2, 0\}$	$Q=e_0+e_1\mathbf{i}+e_2\mathbf{j}+e_3\mathbf{k}+\varepsilon(g_1\mathbf{i}+g_2\mathbf{j})$			Spherical motion and translations along the *X*-axis, *Y*-axis and *Z*-axis with translational distance $2e_0g_1-2e_3g_2$, $2e_0g_2+2e_3g_1$ and $2e_1g_2-2e_2g_1$ respectively.
122	$\{e_0, e_1, e_2, e_3; 0, g_1, 0, g_3\}$	$Q=e_0+e_1\mathbf{i}+e_2\mathbf{j}+e_3\mathbf{k}+\varepsilon(g_1\mathbf{i}+g_3\mathbf{k})$			Spherical motion and translations along the *X*-axis, *Y*-axis and *Z*-axis with translational distance $2e_0g_1+2e_2g_3$, $-2e_1g_3+2e_3g_1$ and $2e_0g_3-2e_2g_1$ respectively.
123	$\{e_0, e_1, e_2, e_3; 0, 0, g_2, g_3\}$	$Q=e_0+e_1\mathbf{i}+e_2\mathbf{j}+e_3\mathbf{k}+\varepsilon(g_2\mathbf{j}+g_3\mathbf{k})$			Spherical motion and translations along the *X*-axis, *Y*-axis and *Z*-axis with translational distance $2e_2g_3-2e_3g_2$, $2e_0g_2-2e_1g_3$ and $2e_0g_3+2e_1g_2$ respectively.
124	$\{e_0, e_1, e_2, 0; g_0, g_1, g_2, g_3\}$	$Q=e_0+e_1\mathbf{i}+e_2\mathbf{j}+\varepsilon(g_0+g_1\mathbf{i}+g_2\mathbf{j}+g_3\mathbf{k})=(-e_2\mathbf{i}+e_1\mathbf{j}-e_0\mathbf{k})\mathbf{k}+\varepsilon(g_0+g_1\mathbf{i}+g_2\mathbf{j}+g_3\mathbf{k})$	2	3	Half-turn rotation about the *Z*-axis followed by a half-turn rotation about the axis $\boldsymbol{u}=(-e_2, e_1, -e_0)^T$, and translations along the *X*-axis, *Y*-axis and *Z*-axis with translational distance $2e_0g_1-2e_1g_0+2e_2g_3$, $2e_0g_2-2e_1g_3-2e_2g_0$ and $2e_0g_3+2e_1g_2-2e_2g_1$ respectively.
125	$\{e_0, e_1, 0, e_3; g_0, g_1, g_2, g_3\}$	$Q=e_0+e_1\mathbf{i}+e_3\mathbf{k}+\varepsilon(g_0+g_1\mathbf{i}+g_2\mathbf{j}+g_3\mathbf{k})=(e_3\mathbf{i}-e_0\mathbf{j}-e_1\mathbf{k})\mathbf{j}+\varepsilon(g_0+g_1\mathbf{i}+g_2\mathbf{j}+g_3\mathbf{k})$			Half-turn rotation about the *Y*-axis followed by a half-turn rotation about the axis $\boldsymbol{u}=(e_3, -e_0, -e_1)^T$, and translations along the *X*-axis, *Y*-axis and *Z*-axis with translational distance $2e_0g_1-2e_1g_0-2e_3g_2$, $2e_0g_2-2e_1g_3+2e_3g_1$ and $2e_0g_3+2e_1g_2-2e_3g_0$ respectively.
126	$\{e_0, 0, e_2, e_3; g_0, g_1, g_2, g_3\}$	$Q=e_0+e_2\mathbf{j}+e_3\mathbf{k}+\varepsilon(g_0+g_1\mathbf{i}+g_2\mathbf{j}+g_3\mathbf{k})=(-e_0\mathbf{i}-e_3\mathbf{j}+e_2\mathbf{k})\mathbf{i}+\varepsilon(g_0+g_1\mathbf{i}+g_2\mathbf{j}+g_3\mathbf{k})$			Half-turn rotation about the *X*-axis followed by a half-turn rotation about the axis $\boldsymbol{u}=(-e_0, -e_3, e_2)^T$, and translations along the *X*-axis, *Y*-axis and *Z*-axis with translational distance $2e_0g_1+2e_2g_3-2e_3g_2$, $2e_0g_2-2e_2g_0+2e_3g_1$ and $2e_0g_3-2e_2g_1-2e_3g_0$ respectively.
127	$\{0, e_1, e_2, e_3; g_0, g_1, g_2, g_3\}$	$Q=e_1\mathbf{i}+e_2\mathbf{j}+e_3\mathbf{k}+\varepsilon(g_0+g_1\mathbf{i}+g_2\mathbf{j}+g_3\mathbf{k})$			Half-turn rotation about the axis $\boldsymbol{u}=(e_1, e_2, e_3)^T$ and translations along the *X*-axis, *Y*-axis and *Z*-axis with translational distance $-2e_1g_0+2e_2g_3-2e_3g_2$, $-2e_1g_3-2e_2g_0+2e_3g_1$ and $2e_1g_2-2e_2g_1-2e_3g_0$ respectively.
128	$\{e_0, e_1, e_2, e_3; g_0, g_1, g_2, 0\}$	$Q=e_0+e_1\mathbf{i}+e_2\mathbf{j}+e_3\mathbf{k}+\varepsilon(g_0+g_1\mathbf{i}+g_2\mathbf{j})$	3	2	Spherical motion and translations along the *X*-axis, *Y*-axis and *Z*-axis with translational distance $2e_0g_1-2e_1g_0-2e_3g_2$, $2e_0g_2-2e_2g_0+2e_3g_1$ and $2e_1g_2-2e_2g_1-2e_3g_0$ respectively.
129	$\{e_0, e_1, e_2, e_3; g_0, g_1, 0, g_3\}$	$Q=e_0+e_1\mathbf{i}+e_2\mathbf{j}+e_3\mathbf{k}+\varepsilon(g_0+g_1\mathbf{i}+g_3\mathbf{k})$			Spherical motion and translations along the *X*-axis, *Y*-axis and *Z*-axis with translational distance $2e_0g_1-2e_1g_0+2e_2g$, $-2e_1g_3-2e_2g_0+2e_3g_1$ and $2e_0g_3-2e_2g_1-2e_3g_0$ respectively.
130	$\{e_0, e_1, e_2, e_3; g_0, 0, g_2, g_3\}$	$Q=e_0+e_1\mathbf{i}+e_2\mathbf{j}+e_3\mathbf{k}+\varepsilon(g_0+g_2\mathbf{j}+g_3\mathbf{k})$			Spherical motion and translations along the *X*-axis, *Y*-axis and *Z*-axis with translational distance $-2e_1g_0+2e_2g_3-2e_3g_2$, $2e_0g_2-2e_1g_3-2e_2g_0$ and $2e_0g_3+2e_1g_2-2e_3g_0$ respectively.
131	$\{e_0, e_1, e_2, e_3; 0, g_1, g_2, g_3\}$	$Q=e_0+e_1\mathbf{i}+e_2\mathbf{j}+e_3\mathbf{k}+\varepsilon(g_1\mathbf{i}+g_2\mathbf{j}+g_3\mathbf{k})$			Spherical motion and translations along the *X*-axis, *Y*-axis and *Z*-axis with translational distance $2e_0g_1+2e_2g_3-2e_3g_2$, $2e_0g_2-2e_1g_3+2e_3g_1$ and $2e_0g_3+2e_1g_2-2e_2g_1$ respectively.
132	$\{e_0, e_1, e_2, e_3; g_0, g_1, g_2, g_3\}$	$Q=e_0+e_1\mathbf{i}+e_2\mathbf{j}+e_3\mathbf{k}+\varepsilon(g_0+g_1\mathbf{i}+g_2\mathbf{j}+g_3\mathbf{k})$	3	3	Spherical motion and translations along the *X*-axis, *Y*-axis and *Z*-axis with translational distance $2e_0g_1-2e_1g_0+2e_2g_3-2e_3g_2$, $2e_0g_2-2e_1g_3-2e_2g_0+2e_3g_1$ and $2e_0g_3+2e_1g_2-2e_2g_1-2e_3g_0$ respectively.

Note: $e_0g_0+e_1g_1+e_2g_2+e_3g_3=0$, $e_0^2+e_1^2+e_2^2+e_3^2=1$.

References

[1]. Q. Li, J.M. Hervé, 1T2R parallel mechanisms without parasitic motion, IEEE Trans. Rob. 26 (3) (2010) 401-410.
[2]. T. Sun, X. Huo, Type synthesis of 1T2R parallel mechanisms with parasitic motions, Mech. Mach. Theory 128 (2018) 412–428.
[3]. J.S. Dai, Z. Huang, H. Lipkin, Mobility of overconstrained parallel mechanisms, ASME J. Mech. Des. 128 (1) (2006) 220-229.
[4]. Y.G. Li, H.T. Liu, X.M. Zhao, T. Huang, D.G. Chetwynd, Design of a 3-DOF PKM module for large structural component machining, Mech. Mach. Theory 45 (6) (2010) 941–954.
[5]. G.R. Dunlop, T.P. Jones, Gravity counter balancing of a parallel robot for antenna aiming, in: Proceedings of 6th ISRAM, 1996, pp. 153–158.
[6]. R.D. Gregorio, Kinematics of the 3-RSR wrist, IEEE Trans. Rob. 20 (4) (2004) 750-753.
[7]. D. Leonardis, M. Solazzi, I. Bortone, A. Frisoli, A wearable fingertip haptic device with 3 DoF asymmetric 3-RSR kinematics, in: Proceedings of the 2015 IEEE World Haptics Conference, IEEE, 2015, pp. 388-393.
[8]. X. Kong, C.M. Gosselin, P.L. Richard, Type synthesis of parallel mechanisms with multiple operation modes. ASME J. Mech. Des. 139 (6) (2006) 595-601.
[9]. D. Zlatanov, I.A. Bonev, C.M. Gosselin, Constraint singularities as C-Space singularities, in: J. Lenarčič, F. Thomas (Eds.), Advances in Robot Kinematics—Theory and Applications, Kluwer Academic Publishers, 2002, pp. 183–192.
[10]. G. Gogu, Maximally regular T2R1-type parallel manipulators with bifurcated spatial motion, ASME J. Mech. Robot. 3 (1) (2011) 011010

[11].Q. Li, J.M. Hervé, Parallel mechanisms with bifurcation of Schoenflies motion, IEEE Trans. Rob. 25 (1) (2009) 158–164.
[12].D. Gan, J.S. Dai, Q. Liao, Mobility change in two types of metamorphic parallel mechanisms, ASME J. Mech. Robot. 1 (4) (2009) 041007.
[13].L. Zhang, J.S. Dai, Reconfiguration of spatial metamorphic mechanisms, ASME J. Mech. Robot. 1 (1) (2008) 011012.
[14].P. Fanghella, C. Gallei, E. Gianotti, Parallel robots that change their group of motion, in: J. Lenarčič, B. Roth (Eds.), Advances in Robot Kinematics, Springer, The Netherlands, 2006, pp. 49–56.
[15].S. Refaat, J.M. Hervé, S. Nahavandi, H. Trinh, Two-mode overconstrained three-DOFs rotational-translational linear-motor-based parallel-kinematics mechanism for machine tool applications, Robotica, 25 (2007) 461-466.
[16].D. Gan, J. Dias, L. Seneviratne, Unified kinematics and optimal design of a 3rRPS metamorphic parallel mechanism with a reconfigurable revolute joint, Mech. Mach. Theory, 96(2016) 239-254.
[17].D. Gan, J.S. Dai, J. Dias, L.D. Seneviratne, Variable motion/force transmissibility of a metamorphic parallel mechanism with reconfigurable 3T and 3R motion, ASME J. Mech. Robot. 8 (5) (2016) 051001.
[18].D. Gan, J.S. Dai, J. Dias, L. Seneviratne, Constraint-plane-based synthesis and topology variation of a class of metamorphic parallel mechanisms, Mech. Mach. Theory, 28(10) (2014) 4179-4191.
[19].X. Kong, J. Yu, Type synthesis of two-degrees-of-freedom 3-4R parallel mechanisms with both spherical translation mode and sphere-on-sphere rolling mode, ASME J. Mech. Robot. 7 (4) (2015) 041018.
[20].X. Kong, Type synthesis of 3-DOF parallel manipulators with both a planar operation mode and a spatial translational operation mode, ASME J. Mech. Robot. 5 (4) (2013) 041015.
[21].X. Kong, Reconfiguration analysis of a variable degrees-of-freedom parallel manipulator with both 3-DOF planar and 4-DOF 3T1R operation modes, in: Proceedings of the ASME 2016 International Design Engineering Technical Conferences and Computers and Information in Engineering Conference, American Society of Mechanical Engineers, 2016, pp. V05BT07A047.
[22].X. Kong, Reconfiguration analysis of a 3-DOF parallel mechanism using Euler parameter quaternions and algebraic geometry method, Mech. Mach. Theory, 74 (2014) 188-201.
[23].M. Raghavan, B. Roth, Solving polynomial system for the kinematic analysis and synthesis of mechanisms and robot manipulator, ASME J. Vib. Acoust. 117 (B) (1995) 71-79.
[24].T. Arponen, A. Müller, S. Piipponen, J. Tuomela, Kinematical analysis of overconstrained and underconstrained mechanisms by means of computational algebraic geometry, Meccanica, 49 (2014) 843-862.
[25].T. Arponen, A. Müller, S. Piipponen, J. Tuomela, Computational algebraic geometry and global analysis of regional manipulators, Appl. Math. Comput. 232 (2014) 820-835.
[26].T. Arponen, S. Piipponen, J. Tuomela, Kinematical analysis of Wunderlich mechanism, Mech. Mach. Theory, 70 (2013) 16-31.
[27].J.M. Selig, Geometric Fundamentals of Robotics, Springer, New York, 2005.
[28].J. Schadlbauer, Algebraic methods in kinematics and line geometry, Doctoral thesis, University Innsbruck, 2014.
[29].D.R. Walter, M.L. Husty, M. Pfurner, Chapter A: complete kinematic analysis of the SNU 3-UPU parallel manipulator, Contemporary Mathematics, American Mathematical Society, Vol 496, 2009, pp. 331–346.
[30].T. Stigger, A. Nayak, S. Caro, P. Wenger, M. Pfurner, M. Husty, Algebraic analysis of a 3-RUU parallel manipulator, in: J. Lenarcic, V. Parenti-Castelli (Eds.), Advances in Robot Kinematics 2018, Springer Proceedings in Advanced Robotics, 8, Springer, Cham, Bologna, Italy, 2018, pp. 141–149.
[31].J.J. Yu, Z. Jin, X. Kong, Identification and comparison for continuous motion characteristics of three two-degree-of-freedom pointing mechanisms. ASME J. Mech. Robot. 9(5) (2017) 051015.
[32].J. Schadlbauer, D.R. Walter, M.L. Husty, The 3-RPS parallel manipulator from an algebraic viewpoint, Mech. Mach. Theory, 75 (2014) 161-176.
[33].A. Nayak, T. Stigger, M.L. Husty, P Wenger, S Caro, Operation mode analysis of 3-RPS parallel manipulators based on their design parameters, Comput. Aided Des. 63 (2018) 122-134.
[34].A. Nayak, S. Caro, P. Wenger, Comparison of 3-[PP]S parallel manipulators based on their singularity free orientation workspace, parasitic motions and complexity, Mech. Mach. Theory, 129 (2018) 293-315.
[35].J. Schadlbauer, L. Nurahmi, M. Husty, P Wenger, S Caro, Operation modes in lower-mobility parallel manipulators, in: A. Kecskeméthy, F. Geu Flores (eds.), Interdisciplinary Applications in Kinematics, Springer, Cham, Vol. 26, 2015, pp. 1-9.
[36].F. Thomas. Approaching dual quaternions from matrix algebra, IEEE Trans. Rob. 30 (5) (2017) 1037-1048.
[37].E. Bayro-Corrochano, Modeling the 3D kinematics of the eye in the geometric algebra framework, Pattern Recognit. 36 (12) (2003) 2993-3012.
[38].R.D. Gregorio, Inverse position analysis, workspace determination and position synthesis of parallel manipulators with 3-RSR topology, Robotica 21 (2003) 627-632.
[39].I.A. Bonev, D. Zlatanov, C.M. Gosselin, Advantages of the modified euler angles in the design and control of PKMs, in: Proceedings of the 3rd Chemnitz parallel kinematics seminar, Chemnitz, Germany, 2002, pp.199-216.
[40].Z. Chen, H. Ding, W. Cao, Z. Huang, Axodes analysis of the multi DOF parallel mechanisms and parasitic motion, in: Proceedings of the ASME 2013 International Design Engineering Technical Conferences and Computers and Information in Engineering Conference, American Society of Mechanical Engineers, 2013, pp. V06AT07A052.
[41].J.J. Yu, K. Wu, G.H. Zong, X. Kong, A comparative study on motion characteristics of three two-degree-of-freedom pointing mechanisms, ASME J. Mech. Rob. 8 (2) (2016) 021027.
[42].L. Nurahmi, J. Schadlbauer, M. Husty, P. Wenger, S Caro, Motion capability of the 3-RPS cube parallel manipulator, in: J. Lenarčič, O. Khatib (Eds.), Advances in Robot Kinematics, Springer, Cham, 2014, pp. 527-535.
[43].J.M. Selig, M. Husty,, Half-turns and line symmetric motions, Mech. Mach. Theory, 46 (2011) 156-167.
[44].K.H. Hunt, Structural kinematics of in-parallel-actuated robot-arms, ASME J. Mech. Transm. Autom. Des. 105 (4) (1983) 705-712.
[45].X.J. Liu, I.A. Bonev, Orientation capability, error analysis, and dimensional optimization of two articulated tool heads with parallel

Mechanism and Machine Theory, 2019, Vol 142, 103577
https://doi.org/10.1016/j.mechmachtheory.2019.103577

kinematics, ASME J. Manuf. Sci. Eng. 130 (1) (2008) 284-284.